Title

Isopentenyl diphosphate (IPP)-bypass mevalonate pathways for isopentenol production

Authors

Kang, Aram

George, Kevin W

Wang, George

et al.

Publication Date

2016-03-01

DOI

10.1016/j.ymben.2015.12.002

Peer reviewed

Isopentenyl diphosphate (IPP)-bypass mevalonate pathways for isopentenol production

Aram Kang[1,2], Kevin W. George[1,2], George Wang[1,2], Edward Baidoo[1,2], Jay D. Keasling[1,2,3,4], Taek Soon Lee[1,2,*]

[1]Joint BioEnergy Institute, 5885 Hollis Street, Emeryville, CA 94608, USA.

[2]Biological Systems & Engineering Division, Lawrence Berkeley National Laboratory, Berkeley, CA 94720, USA.

[3]Department of Bioengineering, University of California, Berkeley, CA 94720, USA.

[4]Department of Chemical and Biomolecular Engineering, University of California, Berkeley, CA 94720, USA.

[*]Corresponding author: Dr. Taek Soon Lee, Joint BioEnergy Institute, 5885 Hollis St. 4th floor, Emeryville, CA 94608, USA; Phone: +1-510-495-2470, Fax: +1-510-495-2629, E-mail: tslee@lbl.gov

Keywords: Isopentenol, isoprenol, mevalonate pathway, biofuel, phosphomevalonate decarboxylase, IPP, toxicity, aeration

Abstract

Branched C_5 alcohols are promising biofuels with favorable combustion properties. A mevalonate (MVA)-based isoprenoid biosynthetic pathway for C_5 alcohols was constructed in *E. coli* using genes from several organisms, and the pathway was optimized to achieve over 50% theoretical yield. Although the MVA pathway is energetically less efficient than the native methylerythritol 4-phosphate (MEP) pathway, implementing the MVA pathway in bacterial hosts such as *E. coli* is advantageous due to its lack of endogenous regulation. The MVA and MEP pathways intersect at isopentenyl diphosphate (IPP), the direct precursor to isoprenoid-derived C_5 alcohols and initial precursor to longer chain terpenes, which makes independent regulation of the pathways difficult. In pursuit of the complete "decoupling" of the MVA pathway from native cellular regulation, we designed novel IPP-bypass MVA pathways for C_5 alcohol production by utilizing promiscuous activities of two enzymes, phosphomevalonate decarboxylase (PMD) and an *E. coli*-endogenous phosphatase (AphA). These bypass pathways have reduced energetic requirements, are further decoupled from intrinsic regulation, and are free from IPP-related toxicity. In addition to these benefits, we demonstrate that reduced aeration rate has less impact on the bypass pathway than the original MVA pathway. Finally, we showed that performance of the bypass pathway was primarily determined by the activity of PMD. We designed PMD mutants with improved activity and demonstrated titer increases in the mutant strains. These modified pathways would be a good platform for industrial production of isopentenol and related chemicals such as isoprene.

1. Introduction

Isopentenol (3-methyl-3-buten-1-ol) is a potential biofuel and important precursor for flavor compounds (prenols and isoamyl alcohol esters) and industrial chemicals such as isoprene [1,2]. Two classes of metabolic pathways have been engineered to produce isopentenol in microbial hosts: amino acid production pathways utilizing 2-keto-acid intermediates [3,4], and isoprenoid biosynthesis pathways, including both the mevalonate (MVA) [1,5–7] and non-mevalonate pathway (methylerythritol 4-phosphate (MEP) or 1-deoxy-D-xylulose 5-phosphate (DXP) pathway) [8]. A heterologous MVA pathway was constructed to produce isopentenol in *Escherichia coli* by expressing 7 genes (Fig. 1-Pathway O) [1]. To produce isopentenol, IPP is hydrolyzed by phosphatases such as NudF from *Bacillus subtilis* or NudB from *E. coli*. Although the initial performance of this pathway was low (8.3% of pathway-dependent theoretical yield), subsequent optimization has significantly improved yields and titers [6,7]. Most recently, isopentenol was produced at a titer of 2.2 g/L from 10 g/L glucose, which is almost 70% of apparent theoretical yield [9].

A variety of engineering strategies have been applied to optimize the heterologous MVA pathway and improve isoprenoid production in *E. coli* [10–15]. In each case, balanced expression of pathway enzymes was required to maximize flux towards final products while minimizing the accumulation of toxic intermediates such as farnesyl diphosphate (FPP) [16], IPP [5–7,16], and 3-hydroxy-3-methyl-glutaryl-CoA (HMG-CoA) [17]. For isopentenol production, the careful management of IPP levels is critical: engineering strategies to address its accumulation have included the deliberate “tuning”

of the upstream MVA pathway [6] and the extensive overexpression of NudB, the phosphatase required to transform IPP into isopentenol [9].

Although the mechanism of IPP toxicity is unknown, the deleterious effects of its accumulation are clear. First, it has been demonstrated in various studies that accumulation of IPP inhibits cell growth [5,6,16], which prevents a bioprocess from achieving enough cell biomass to maximize product titer. Even prior to affecting cell growth, it is likely that the transient accumulation of IPP induces a variety of stress responses as has previously been observed during the accumulation of FPP [14]. Responses to both generalized (e.g., RpoS-induced [18]) and condition-specific stress (e.g., acid stress [19], oxidative stress [20] and osmotic stress [21]) result in the recruitment of ATP-dependent defense mechanisms including DNA repair [19,20], ATPases [19], and ABC transporters [21]. The ATP cost of these processes may serve to compete with the energetically-expensive MVA pathway, reducing the yield and productivity of isoprenoid production. In the case of isopentenol production, high flux to IPP has an additional detrimental impact: through the action of *E. coli* native IPP isomerase (Idi), IPP can be diverted by native isoprenoid pathways that produce C_{10}- and C_{15}-prenyl diphosphates (i.e. geranyl diphosphate (GPP) and FPP). The production of GPP and FPP decreases the carbon utilization efficiency of isopentenol production, and potentially inhibits MK activity, which in turn reduces MVA flux to the downstream enzyme reactions [22]. Moreover, isopentenol production via IPP requires the energetically expensive ATP-consuming formation of diphosphate prior to enzymatic hydrolysis. This diphosphate formation and subsequent hydrolysis is considerably inefficient in terms of atom and energy economy. Due to these factors, the “IPP-

dependency" of the MVA pathway may intrinsically limit the engineering of the MVA pathway for more efficient isopentenol production.

In this work, we successfully decouple isopentenol production from IPP formation by constructing two novel "IPP-bypass" pathways. These two IPP-bypass pathways rely on decarboxylation of either MVA or MVA monophosphate (MVAP) for isopentenol production and do not produce IPP as an essential precursor for isopentenol. These optimized pathways eliminate the negative effects of IPP accumulation such as growth inhibition, energy-consuming stress responses, diverted carbon flux, and regulatory inhibition on mevalonate kinase (MK). We envision that these two IPP-bypass pathways could open a new dimension of engineering the MVA pathway to produce isopentenol and isopentenol-derived valuable compounds such as isoprene.

2. Materials and Methods

2.1. Strains and plasmid construction

All strains and plasmids used in this study are listed in Table 1. Throughout the studies, *E. coli* BW25113 strain was used for isopentenol production, and *E. coli* DH10B was used for genetic cloning. The original sequence of PMD_{hv} was obtained from NCBI database (HVO_1412, NC_013967.1), codon-optimized for expression in *E. coli* by GenScript (New Jersey, USA), and the optimized sequence was synthesized by IDT (Iowa, USA). A plasmid coding PMD_{se} was received from Dr. Miziorko at University of Missouri [23], and the coding sequence was amplified by PCR for sub-cloning to expression vectors.

2.2. Protein expression and purification

A plasmid encoding a wild type mevalonate diphosphate decarboxylase from *S. cerevisiae* (PMD_{sc}) with N-terminal His-tag (pSKB3-PMD_{sc}) was transformed into *E. coli* BL21 (DE3). A seed culture of BL21 (DE3) harboring pSKB3-PMD_{sc} was prepared by inoculating a single colony and growing it overnight in Luria-Bertani (LB) medium containing kanamycin (50 μg/mL). The seed culture was diluted in Terrific Broth supplemented with 2% glycerol and 50 μg/mL kanamycin and incubated at 37°C until the optical density of the culture at 600 nm (OD_{600}) reached to 0.6-0.8. The cell culture was supplemented with isopropyl-β-D-thiogalactopyranoside (IPTG) to the final concentration of 0.5 mM and transferred to 18°C for protein expression overnight. Cells were collected by centrifugation and re-suspended in 50 mM Tris-HCl (pH 7.5) buffer containing 300 mM NaCl and 10 mM imidazole. Cells were lysed by sonication and purified by HisPur Cobalt Resins (Thermo Scientific, USA). The purified PMD_{sc} was desalted in 10 mM Tris-HCl (pH 7.5) containing 50 mM NaCl, 0.5 mM dithiothreitol (DTT) and 20% glycerol, and flash-frozen in liquid nitrogen for storage at -80°C. All PMD_{sc} mutants, PMD_{se}, and NudB were purified as described above, except that NudB was desalted in 50 mM Tris-HCl (pH 8.0) buffer containing 0.1 mM EDTA, 1 mM DTT and 20% glycerol.

2.3. Enzyme characterization and kinetics

In vitro enzyme kinetics of decarboxylases were performed as described in previous studies [23,24]. Briefly, enzymatic activity of decarboxylase was determined by a spectrophotometer assay quantifying ADP product formation, which was coupled to NADH oxidation by pyruvate kinase/lactate dehydrogenase. Assay mixtures were prepared in 50 mM HEPES-KOH (pH 7.5) containing 10 mM $MgCl_2$, 400 μM

phosphoenolpyruvate, 200 μM NADH, 4 mM ATP, and 25 U of pyruvate kinase/lactate dehydrogenase (Sigma, P0294). The reaction was initiated by addition of various concentrations of MVAP from 100 μM to 4,000 μM, and the reaction velocity was determined by monitoring OD at 340 nm in Spectramax 384plus microplate reader (Molecular Devices, USA).

2.4. Isopentenol production in *E. coli*

E. coli BW25113 harboring two plasmids was used for isopentenol production. Seed cultures of all production strains were prepared by growing single colonies in LB medium containing 100 μg/mL ampicillin and 30 μg/mL chloramphenicol overnight at 37°C with shaking at 200 rpm. The seed cultures were diluted in EZ-Rich defined medium (Teknova, USA) containing 10 g/L glucose (1%, w/v), 100 μg/mL ampicillin and 30 μg/mL chloramphenicol. The *E. coli* cell cultures were incubated in rotary shakers (200 rpm) at 37°C, and 0.5 mM IPTG was added to induce protein expression at OD_{600} of 0.6-0.8. To provide different levels of aeration, identical volumes of the cell culture were split into two flasks for incubation at 30°C with shaking at either 200 rpm or 30 rpm.

For isopentenol quantification, 250 μL of cell culture was combined with 250 μL of ethyl acetate containing 1-butanol (30 mg/L) as an internal standard. This mixture of ethyl acetate and cell culture was vigorously shaken for 15 min and subsequently centrifuged at 13,000 g for 2 min to separate ethyl acetate from the aqueous phase. 100 μL of the ethyl acetate layer was diluted 5-fold, and 1 μL was analyzed by Agilent GCMS equipped with Cyclosil-B column (Agilent, USA) or Thermo GCFID equipped with DB-WAX column (Agilent, USA) for quantitation of isopentenol.

2.5. Phosphatase screening

To identify IP-hydrolyzing endogenous phosphatases, single gene knockout mutants of 36 phosphatases, of which substrates are mostly mono-phosphorylated metabolites, were retrieved from the Keio collection [25]. 1 mL overnight cultures from each mutant were concentrated in 0.5 mL of 50 mM Tris-HCl (pH 8.0) buffer containing 1 mM DTT and ~50 mg of glass beads (< 100 μm, Sigma-Aldrich, USA). Cells were lysed by bead-beating for 2 min at 6.0 M/s (MP biomedicals Fast Prep, USA). After centrifugation of cell lysates at 20,000 g for 10 min, clear supernatant was used for assay reaction containing 0.5 mM isopentenyl monophosphate (IP). An equal volume of ethyl acetate was added to 100 μL of assay reaction after incubating overnight at 30°C, and isopentenol was extracted for 10 min by vigorous mixing.

Coding sequences of *agp*, *aphA*, and *yqaB* were amplified from BW25113 genome by PCR, and they were subsequently cloned to pBbE1a vector [26] for over-expression. All primers used in this study are listed in Supplementary Table 1. Expression of these three genes were induced by addition of 0.5 mM IPTG to the cell cultures, and cell lysates of each sample were prepared with three biological replicates as described above for screening of the 36 mutants. 600 μL of assay reactions containing cell lysates, 1 mM DTT were prepared and the reaction was initiated by addition of 0.5 mM IP. At each time point (0, 1, 3, 6 and 22 hrs), 100 μL of the reaction mixture was sampled and combined with 100 μL of ethyl acetate to extract isopentenol.

2.6. Quantification of metabolites

All metabolites were analyzed by liquid chromatography mass spectrometry (LC-MS; Agilent Technologies 1200 Series HPLC system and Agilent Technologies 6210

time-of-flight mass spectrometer) on a ZIC-HILIC column (150 mm length, 2.1-mm internal diameter, and 3.5-µm particle size). Standard chemicals (IPP and IP) were purchased from Sigma-Aldrich (USA). Metabolites were eluted isocratically with a mobile phase composition of 64% (v/v) acetonitrile containing 50 mM ammonium acetate with a flow rate of 0.15 mL/min. IPP and IP from *E. coli* extracts or enzyme assay were quantified via eight-point calibration curves ranging from 781.25 nM to 200 µM.

3. Results and Discussions

3.1. Design rationale for IPP-bypass isopentenol pathways

The biosynthesis of IPP from MVA consists of three energy-consuming reactions: two kinases (MK and phosphomevalonate kinase (PMK)) result in the formation of diphosphomevalonate (MVAPP), which is subsequently transformed by a decarboxylase (PMD) to form IPP. The diphosphate group of IPP is essential in chain elongation to produce GPP and FPP, and in the carbocation formation to produce cyclic terpenes since the removal of the diphosphate group is thermodynamically-favorable [27]. In isopentenol production via the MVA pathway, the alcohol is also produced by removal of the diphosphate group of IPP. However, this reaction is different from carbocation formation and does not require the diphosphate group as an essential leaving group to drive the hydrolysis reaction. Therefore, formation of the diphosphate group and its subsequent removal make the overall MVA pathway for isopentenol inefficient by unnecessarily consuming two ATPs.

To address the energetic limitations of IPP formation—and the deleterious effects of its accumulation—we designed two modified isopentenol pathways that bypass the

formation of IPP (Fig. 1). The first modified pathway (pathway I) is designed for the direct conversion of MVA to isopentenol via ATP-driven decarboxylative elimination, and the second pathway (pathway II) is designed for a decarboxylative elimination of MVAP to IP followed by the hydrolysis of IP to isopentenol (Fig. 1). These modified pathways result in IPP-independent isopentenol production, which could relieve toxicity and prevent the loss of IPP flux to native pathways such as ubiquinone biosynthesis. Moreover, these two pathways reduce the complexity and energy cost of isopentenol production. As shown in Fig 1, direct decarboxylation of MVA (pathway I) reduces the number of enzymes required from 7 to 4 and the ATP requirement per molecule of isopentenol from 3 to 1. In IPP-bypass pathway II, the number of enzymes is reduced from 7 to 5 and ATP molecules from 3 to 2 compared to the original pathway. Given the potential benefits of pathways I and II over the original MVA pathway (pathway O), we explored options to construct and express these optimized pathways in *E. coli* to produce isopentenol.

3.2. Engineering of IPP-bypass pathway I and identification of promiscuous decarboxylase activity toward MVA and MVAP

Engineering IPP-bypass pathways I and II requires a decarboxylase that converts MVA or MVAP to isopentenol or IP, respectively. Based on the chemical structures of the substrates and products (Fig. 1) and proposed mechanism of the decarboxylation reaction, we hypothesized that PMD might serve as a decarboxylase for MVA and MVAP in addition to its native substrate, MVAPP. Since PMD from *S. cerevisiae* (PMD_{sc}) has been widely used for isoprenoid production in engineered *E. coli* [6,7,28–30], we initially chose PMD_{sc} as the target PMD enzyme for each bypass pathway.

PMD_{sc} was previously reported to convert 3-hydroxy-3-methylbutyrate (3-HMB) to isobutene [31], which supports the hypothesis that this enzyme has promiscuous decarboxylase activity.

With PMD_{sc} as a potential decarboxylase for MVA, IPP-bypass pathway I was first constructed in *E. coli* by expressing three enzymes (AtoB, HMGS, and HMGR) to produce MVA along with PMD_{sc} (strain ARK3a, Table 1). When the strain was tested *in vivo*, the engineered *E. coli* produced 0.85±0.18 mg/L isopentenol (Fig. 2B) while the control strain, which expressed only AtoB, HMGS, and HMGR without PMD_{sc} (strain ARK3b, Table 1) did not show any detectable level of isopentenol (Fig. 2A). The fragmentation pattern and retention time of the isopentenol peak detected in strain ARK3a matched those from a 3-methyl-3-buten-1-ol standard (Fig. 2C). *In vitro* activity measurement was attempted to determine the kinetic parameters of PMD_{sc} for MVA, but the enzyme activity was too low to determine the kinetic parameters (data not shown).

Structural analysis of a homologous PMD from *Staphylococcus epidermis* (PMD_{se}) [23] suggested that the diphosphate group is important for substrate binding even though it is not directly involved in the catalytic decarboxylation reaction (Supplementary Fig. S1). The importance of the diphosphate group in PMD_{se} activity implies that the monophosphorylated substrate (i.e. MVAP) might be better suited for decarboxylation than the substrate without any phosphate group (i.e. MVA).

3.3. Engineering of IPP-bypass pathway II and pathway optimization in *E. coli*

To verify the improved activity of PMD_{sc} for phosphorylated substrates (MVAP), an *in vitro* assay was performed with both MVA and MVAP. While isopentenol was not detected in the *in vitro* reaction, a detectable amount of IP was produced when MVAP

was used as a substrate for PMD_{sc}. This result indicates that PMD_{sc} has higher decarboxylase activity towards MVAP than MVA and suggests that the phosphate group of MVAP does indeed enhance substrate binding and catalysis (Supplementary Fig. S1). The k_{cat} (0.14 s^{-1}) and K_m (0.99 mM) of PMD_{sc} toward MVAP (Supplementary Fig. S2), were about 35-fold lower and 8-fold higher than the reported k_{cat} (4.9 sec^{-1}) and K_m (123 μM) toward the native substrate (MVAPP), respectively [32].

With a confirmation of promiscuous PMD_{sc} activity for MVAP, we constructed a new IPP-bypass pathway (pathway II in Fig. 1) by expressing AtoB, HMGS, HMGR, MK, and PMD_{sc} in *E. coli* (strain ARK2a, Table 1). Strain ARK2a produced 474.7 mg/L of isopentenol, a 558-fold improvement over the strain with pathway I (strain ARK3a). This new strain (strain ARK2a) achieved about 62.4% of the titer of the original isopentenol pathway (pathway O with strain ARK1a). It is noteworthy that IPP-bypass pathway II could produce isopentenol even without over-expressing any additional phosphatase that would hydrolyze the phosphate group in IP, which will be discussed in detail in the next section.

3.4. Identification of endogenous phosphatase for IP

The successful production of isopentenol via IPP-bypass pathway II suggested that endogenous *E. coli* phosphatases are capable of hydrolyzing IP to isopentenol. Initially, we hypothesized that IP might be hydrolyzed by promiscuous activities of Nudix hydrolases such as NudB in *E. coli* or an *E. coli* homolog of *B. subtilis* NudF, both of which were previously used to convert IPP to isopentenol [1,5]. In the original IPP-dependent isopentenol pathway, the expression of NudB or NudF was essential for isopentenol production from IPP, and *in vitro* kinetic experiments of NudB showed that

IPP was hydrolyzed by the enzyme [1]. However, the previous assay was based on the detection of the monophosphate formation without analyzing the final product by LCMS or GCMS, and it was not determined whether NudB hydrolyzes IPP by two consecutive hydrolysis reactions of two monophosphates or by a single hydrolysis reaction of a diphosphate group. We hypothesized that if NudB hydrolyzes IPP via the former fashion (i.e. two consecutive hydrolyses), both IP (intermediate) and isopentenol would be detected from an *in vitro* assay containing purified NudB and IPP. Interestingly, an *in vitro* assay of purified NudB with IPP produced only IP—no isopentenol was detected even after an extended incubation of 16 hours (Fig. 3A). Similarly, purified NudB could hydrolyze DMAPP to DMAP, but the final hydrolysis product, 3-methyl-2-butenol, was not detected (Supplementary Fig. S3A). In addition to NudB, NudF of *B. subtilis*, which was identified as a IPP hydrolase in a previous study [5], was also found to hydrolyze IPP to IP, but not to isopentenol (Supplementary Fig. S3B). On the other hand, it was confirmed *in vitro* that crude cell lysates of *E. coli* did hydrolyze IP to isopentenol (Fig. 3B). This result suggests that in the original isopentenol pathway, NudB hydrolyzed IPP to IP, but the following hydrolysis of IP to isopentenol was catalyzed by unknown endogenous phosphatase(s) in *E. coli*.

To identify the unknown endogenous phosphatase(s), phosphatase single gene knockout mutants were tested for their capability to hydrolyze IP to isopentenol. We reasoned IP hydrolysis to isopentenol would significantly decrease if the responsible IP-hydrolyzing enzyme was absent in the knockout mutant strain. A total of 36 monophosphatase single gene knockout mutant strains were obtained from the Keio collection [25], and cell lysate from each individual strain was incubated with IP *in vitro*.

299 Cell lysates from three single gene knockout mutant strains (Δ*agp*, Δ*aphA* and Δ*yqaB*)
300 produced significantly less isopentenol than the average level of isopentenol produced by
301 all strains tested including the wild type (Fig. 4A). Even after 26 hours of incubation, the
302 relative isopentenol level produced from cell lysates of Δ*agp*, Δ*aphA* and Δ*yqaB* mutants
303 were only 62%, 64% and 82% of the level from the wild type, respectively (Fig. 4B). It
304 is noteworthy that cell lysates of all 36 mutants has some IP-hydrolyzing activity,
305 suggesting that multiple endogenous phosphatases capable of hydrolyzing IP.

306 IP-hydrolysis efficiency significantly increased when one of these three genes,
307 *aphA*, was overexpressed both in wild type and in the *aphA*-knockout mutant. In these
308 strains, IP was completely converted into isopentenol immediately after addition of the IP
309 to hydrolysates reactions (Fig. 4C). On the other hand, overexpression of the other two
310 genes (*agp* and *yqaB*) showed relatively much slower IP hydrolysis rates (Fig. 4C),
311 suggesting that *aphA* has much higher IP-hydrolysis activity than those of *agp* and *yqaB*.
312 Co-expression of *aphA* along with pathway II (AtoB, HMGS, HMGR, MK and PMD_{sc};
313 strain ARK2aa) resulted in an isopentenol titer of 705 mg/L after 31 hours of incubation,
314 which is about 20% higher than that of the strain without *aphA* overexpression (strain
315 ARK2a; Fig. 5) and 83% of the maximum titer of the original isopentenol pathway
316 (pathway O in Fig. 1; strain ARK1a in Table 1; 836.9 mg/L). Although AphA is a
317 membrane-bound protein whose overexpression frequently is detrimental and inhibits
318 growth [33], there was no significant growth difference between strains with or without
319 *aphA*-overexpression (strains ARK2aa and ARK2a, respectively). Achieving a
320 significant improvement in conversion of IP to isopentenol by *aphA* overexpression, we
321 reasoned that the overall flux to isopentenol in strain ARK2aa could be further improved

by increasing the activity of PMD_{sc} toward MVAP. We thus focused on improving the promiscuous activity of PMD_{sc} toward non-native substrates.

3.5. PMD engineering for improved activity toward mevalonate monophosphate

To engineer the active site of PMD_{sc} for the non-native substrate MVAP, we first identified amino acid residues in PMD putatively responsible for binding the native substrate (MVAPP). Since the only X-ray crystal structure of PMD_{sc} was solved without a bound substrate [34], the coordinates of MVAPP in the active site of PMD_{sc} were predicted by aligning the crystal structure of PMD_{sc} (PDB#: 1FI4) to that of the homologous PMD enzyme from *S. epidermis* (PMD_{se}, PDB#: 4DPT) (Supplementary Fig. S4A). Crystal structures of PMD_{se} were solved with two substrate analogs: adenosine 5-[γ-thio]triphosphate (ATPγS) and 6-fluoromevalonate 5-diphosphate (FMVAPP) [23]. Alignment of PMD_{sc} and PMD_{se} amino acid sequences showed 50% similarity by BLAST search and revealed conserved residues for catalysis and substrate binding (Supplementary Fig. S4B). However, *in vivo* isopentenol production with IPP-bypass pathway II and PMD_{se} (strain ARK4) was significantly reduced relative to PMD_{sc} (11.3 mg/L vs 474.7 mg/L after 24 hrs), suggesting that the activity of PMD_{se} toward MVAP could be much lower than that of PMD_{sc}. The k_{cat}/K_m ratios of PMD_{sc} and PMD_{se} are 4.0×10^4 s^{-1} M^{-1} [32] and 6.5×10^5 s^{-1} M^{-1} [23], respectively, which indicates higher substrate specificity of PMD_{se} for MVAPP. Increased substrate specificity in PMD_{se} could be attributed to the positively charged arginine at residue 193 (R193) [23]. R193 of PMD_{se} is located within hydrogen bonding distance of the β-phosphate moiety of MVAPP and stabilizes the binding of MVAPP to the enzyme. On the other hand, PMD_{sc} has a neutral threonine residue in the homologous position (T209) instead of the

positively charged arginine (Supplementary Fig. S4B), and this perhaps allows the promiscuity of PMD_{sc} towards the less negatively charged MVAP.

After we engineered the bypass pathway II with PMD_{sc}, an archaeal MVAP-specific decarboxylase was identified in *Haloferax volcanii* (PMD_{hv}) with much better kinetics for MVAP (K_m of 0.159 mM and k_{cat} of 3.5 s^{-1} for MVAP; and no activity toward MVAPP) [24]. Unlike the conventional MVA pathway that supplies IPP via decarboxylation of MVAPP, the archaeal MVA pathway produces IPP via phosphorylation of IP, which is produced by decarboxylation reaction of MVAP similar to our bypass pathway II. Therefore, PMD_{hv} was expected to be a natural decarboxylase that can convert MVAP to IP in the IPP-bypass pathway II. Surprisingly, however, no isopentenol production was detected when four pathway genes in the bypass pathway II (AtoB, HMGS, HMGR and MK) were expressed *in vivo* along with PMD_{hv} (strain ARK5; data not shown). An ATP-NADH coupled assay was also performed *in vitro* to detect the activity of PMD_{hv} toward MVAP, but no ATP hydrolysis activity was observed either. In the previous work where PMD_{hv} kinetics were determined, PMD_{hv} was overexpressed in its native host, *H. volcanii*, at 42 °C in salt-rich Hv-YPC media (containing 144 g of NaCl, 21 g of $MgSO_4 \bullet 7H_2O$, 18 g of $MgCl_2 \bullet 6H_2O$ and 4.2 g of KCl) [24]. Given that optimal growth temperatures and salt concentration in media of *H. volcanii* are different from those for *E. coli*, PMD_{hv} could have been expressed but inactive in *E. coli*. Nonetheless, it was noteworthy that four residues from PMD_{sc} that interact with β-phosphates of MVAPP were missing in PMD_{hv} between threonine 186 (T186) and glutamate 187 (E187) [24]. In other homologous PMD sequences from species with conventional MVA pathways, these missing residues are rich in serine and

368 arginine, which facilitates interaction with the phosphoryl moieties of MVAPP and ATP.
369 Therefore, analysis of residues near β-phosphate of MVAPP in three PMDs suggested
370 that the activity of PMD_{sc} toward MVAP could be improved by re-designing the local
371 electrostatic environment around the β-phosphate of MVAPP.

372 Based on structural analysis of these three PMDs (PMD_{sc}, PMD_{se} and PMD_{hv}),
373 four residues (K22, S155, S208 and T209) of PMD_{sc} adjacent to the β-phosphate of the
374 MVAPP were selected for engineering (Supplementary Fig. S5). While the original
375 substrate MVAPP has a net charge of -4, two alternative substrates, MVAP and MVA,
376 have a net charge of -2 and 0, respectively. To compensate for this reduced negative
377 charge, two serine residues (S155 and S208) were mutated to negatively charged
378 glutamate (E), and the other two residues near the phosphate moiety (K22 and T209)
379 were mutated to neutral methionine (M) and negatively charged aspartate (D),
380 respectively. In addition, we constructed two more mutants, R74H and I145F (Fig. 6A),
381 which were previously shown to increase activity of PMD_{sc} in the similar
382 decarboxylation reaction for 3-hydroxy-3-methylbutyrate (3-HMB) to produce isobutene
383 [31]. *In vitro* assay reactions using cell lysates of two serine-to-glutamate mutations
384 (S155E and S208E) did not produce detectible amount of product, which suggests that
385 these two mutations significantly reduced the activity of PMD_{sc} toward MVAP unlike the
386 other mutants (data not shown). The K22M mutation increased K_m and decreased k_{cat},
387 but the kinetic parameters of the T209D mutant were similar to those of the wild type
388 (Table 2, Fig. 6B). Interestingly, the specificity of PMD_{sc} toward MVAP (k_{cat}/K_m) with
389 R74H or I145F mutation was 220% and 147% of that of wild type, respectively.
390 Although R74 and I145 are located near the active site, it is unlikely that these residues

391 interact directly with substrates: distances from the α-phosphate group of MVAPP are
392 12.5 Å and 15.0 Å, respectively (Fig. 6A). Therefore, the improved activity of the R74H
393 and I145F mutants toward MVAP and 3-HMB suggests that these two mutations changed
394 the conformation of the active site to accommodate less negatively charged substrates.
395 Although R74H and I145F increased activity for MVAP and 3-HMB, two mutants did
396 not show detectible hydrolysis activity on MVA.

397 After identifying two mutations in PMD_{sc} that improve activity toward MVAP,
398 we prepared *E. coli* strains overexpressing four enzymes (AtoB, HMGS, HMGR, MK)
399 along with one of three different PMD mutants including R74H (stain $ARK2a_{M1}$), I145F
400 (strain $ARK2a_{M2}$), or the double mutant (strain $ARK2a_{M3}$) to see whether improved
401 specificity for MVAP would increase isopentenol production in IPP-bypass pathway II.
402 As shown in Fig. 6C, R74H (strain $ARK2a_{M1}$) resulted in significantly improved
403 productivity (20.4 mg/L/hr) over wild type (15.9 mg/L/hr) through 30 hours of batch
404 fermentation. The I145F mutation (strain $ARK2a_{M2}$), however, reduced isopentenol titer
405 and productivity *in vivo* even though this mutation improved *in vitro* enzyme activity
406 (Table 2). Interestingly, when these two mutations were combined (strain ARK $2a_{M3}$),
407 the titer and productivity were recovered to the comparable level to those of R74H, which
408 suggests that R74H mutation was dominant over the I145F mutation.

409 Successful identification of PMD mutants that improve or significantly reduce
410 isopentenol titer and productivity supports the hypothesis that the promiscuous activity of
411 PMD toward MVAP is the current bottleneck of the IPP-bypass pathway II. Given the
412 huge engineering space to explore various mutations that can potentially improve the

activity of PMD toward MVAP, this result provides a clear opportunity to improve IPP-bypass pathway II for isopentenol production.

3.6. Effect of MVA levels on isopentenol production in the IPP-bypass pathway II

We successfully engineered IPP-bypass MVA pathways for isopentenol production and showed that pathway II could be improved by facilitating two limiting reactions: hydrolysis of IP and decarboxylation of MVAP to IP. Next, we targeted the "top" portion of the MVA pathway with engineering that would modulate pathway flux to MVA and tested how this variation affects isopentenol production in IPP-bypass pathway II. Previously, heterologous MVA pathways were constructed and tested with various combinations of HMGS and HMGR, and different pairs of HMGS-HMGR resulted in different levels of MVA and final isoprenoid titers [6,10,17,22]. The MVA level was reported to affect MK activity by substrate inhibition [22], and therefore, optimizing MVA flux has been one approach to improve titers of isoprenoid products.

To evaluate the effects of MVA concentration in IPP-bypass pathway II, we reconstructed the original and the modified pathways with four different pairs of HMGS and HMGR in the "top" portion of the pathway (Fig. 1): non-codon optimized original sequences from *S. cerevisiae* genes (MevTo), *E. coli*-codon optimized sequences of *S. cerevisiae* genes (MevTco), HMGS and HMGR of *Staphylococcus aureus* (MTSA), and those of *Delftia acidovorans* (MTDA).

In accordance with the previous reports, the original IPP-dependent isopentenol pathways showed different isopentenol titers depending on which pairs of HMGS and HMGR were used (Fig. 7). Analysis of intracellular metabolites confirmed that expression of different pairs of HMGS and HMGR indeed resulted in various

intracellular MVA concentrations in strains with both pathway O and pathway II (Supplementary Fig. S6A). Intriguingly, isopentenol titers from the strains containing IPP-bypass pathway II did not change much when the pairs of HMGR and HMGS are changed (Fig. 7), and similar levels of IP were also observed in the strains with pathway II (Supplementary Fig. S6D). This "insensitivity" of the isopentenol titer to various "top" portions and a similar level of IP in pathway II strains suggests that the determining factor of isopentenol production in pathway II could be the PMD activity toward MVAP rather than upstream pathway efficiency.

In addition, metabolite analysis showed that strains with pathway O or pathway II accumulated significantly high levels of IPP or MVAP, respectively, regardless of intracellular MVA concentrations (Supplementary Fig. S6). Interestingly, MVAP was accumulated to considerably higher concentrations than that of IPP (100~200 mM for MVAP vs 30~60 mM for IPP) without any significant toxicity, which is consistent with the previous report that MVAP is not inhibitory to cell growth [16].

3.7. Relief of IPP-toxicity in the bypass pathway II

Previous studies showed that the performance of the original MVA pathway was sensitive to MK expression levels: low MK expression resulted in attenuated flux to IPP and isopentenol, but high levels led IPP accumulation and resulted in growth inhibition [6,9]. Interestingly, growth was restored when NudB was overexpressed in IPP-accumulating strain to relieve IPP-toxicity. In the current study, we demonstrated that NudB could hydrolyze IPP to IP, but not further to isopentenol (Fig. 3), suggesting that IPP has more detrimental effects on growth than does IP.

Since the bypass pathway II does not produce IPP, we hypothesized that the pathway would be insensitive to changes in MK expression and free from related toxicity. To compare growth and isopentenol production in the original and IPP-bypass pathway (pathway O and pathway II) under IPP- or IP-accumulating conditions, respectively, two modifications were made to the strains ARK1a and ARK2a (Supplementary Fig. S7). First, to achieve a moderate level of MK expression in the control strains, we removed the promoter previous added for MK overexpression in the medium copy plasmids JBEI-12056 and JBEI-9310. With this engineering, MK was expressed at a moderate level as the forth enzyme in the operon containing three enzymes for the top portion of the MVA pathway, and it resulted strains ARK1e (harboring JBEI-6818 and JBEI-6833) and ARK2e (harboring JBEI-12051 and JBEI-9314). Second, to achieve very high MK expression level, an additional copy of MK was added to the high copy plasmids, JBEI-6833 and JBEI-9314, resulting ARK1f and ARK2f, respectively (Supplementary Fig. S7). Confirming the previous results [6], balancing flux in the upstream pathway was critical for growth and isopentenol production (Fig. 8). Growth and isopentenol production of ARK1f was significantly reduced showing sensitivity to expression levels of MK, but strains with pathway II was insensitive to down-regulation (ARK2f) or up-regulation (ARK2e) of MK, and free from burden of IPP accumulation (Fig. 8).

3.8. The effect of limited aeration on isopentenol production via IPP-bypass pathway

After characterizing the IPP-bypass pathway II in *E. coli* (strain ARK2a), we tested whether this pathway would have any advantage over the original pathway under ATP-limited conditions. In general, ATP is most efficiently supplied via oxidative phosphorylation with oxygen as a final electron acceptor. As a result, aeration has been

an important operation in industrial-scale fermentation, especially when ATP-demanding isoprenoid biosynthetic pathways are exploited. However, the aeration cost is usually one of the largest portions (up to 26%) of the overall utility cost, and the cost would be on the order of $60 million per year in a plant that processes 2000 MT of dry biomass per day [35]. Moreover, oxygen mass transfer is limited in large-scale fermenters, and this potentially creates a local micro-aerobic or anaerobic environment during fermentation. Therefore, the development of fermentation processes with reduced aeration rates can significantly reduce production cost and improve process efficiency. With this goal in mind, we investigated the impact of reduced aeration on isopentenol production with pathways O and II, which require 3 ATPs and 2 ATPs, respectively, to produce one molecule of isopentenol. To provide different aeration rates, we prepared a 50-mL cell culture with an OD_{600} of 0.6-0.7, split into two 25-mL cell cultures in 250-mL flasks, and continued to incubate at 30°C for induction (0.5 mM IPTG) at two different shaking speeds (30 rpm and 200 rpm).

Fig. 9A shows that the isopentenol titer of pathway O (strain ARK1a) was more significantly affected when aeration was limited by lowering the shaking speed from 200 rpm to 30 rpm. With a reduced aeration, strain ARK1a produced only 22% of the initial titer at 200 rpm after 16 hr-fermentation (Fig. 9B). The bypass pathway II (strain ARK2a), however, produced 40% at 16 hrs and up to 60% of the titers under the higher aeration conditions at 24 hrs. It is noteworthy that the OD_{600} of strain ARK1a was higher than that of strain ARK2a under poor aeration condition (at 30 rpm). A better growth but significantly less isopentenol production of strain ARK1a suggests that the heterologous MVA pathway may compete for ATP with other essential cellular processes related to the

505 growth, and when ATP supply is limited (i.e. under poor aeration conditions), strain
506 ARK1a might reduce the carbon flux to the MVA pathway to reduce the energy usage for
507 this ATP-consuming heterologous pathway. The strain with pathway II (strain ARK2a),
508 however, produced a similar or even higher level of isopentenol under limited aeration
509 conditions after 16 hrs or 24 hrs of fermentation, respectively (Fig. 9A and
510 Supplementary Fig. S8). This result also suggests that the bypass pathway II would be
511 more robust when aeration is limited, and a reduced ATP demand in strain ARK2a is
512 possibly beneficial to the strain under oxygen-limited conditions. Therefore, more
513 economic production of isopentenol could be feasible via the ATP-saving IPP-bypass
514 pathway II by reducing aeration costs for large scale fermentation.

515 ## 4. Conclusion

516 Isopentenol is a potential gasoline alternative and a precursor of commodity
517 chemicals such as isoprene. In this study, we reported our efforts to remove "IPP-
518 dependency" of the original MVA pathway and to overcome limitations intrinsic to IPP
519 accumulation and "unnecessary" consumption of ATPs for isopentenol production. By
520 implementing two previously unidentified activities of PMD_{sc} and AphA, we
521 demonstrated that considerable isopentenol titers could be achieved without producing
522 IPP via the pathway II.

523 The IPP-bypass pathway II was shown to be a robust alternative to the original
524 pathway (pathway O) for isopentenol production. This modified pathway was insensitive
525 to both MVA level and MK expression level, and reduced the engineering burden to
526 balance the upstream MVA pathway and IPP toxicity. Most significantly, the IPP-bypass

pathway II was more competitive when aeration was limited, which would significantly lower operational costs for aeration in a large scale fermentation.

Finally, in this report, we found that the promiscuous activity PMD is rate-limiting. The identification of PMD as the rate-limiting step in these bypass pathways provides clear engineering opportunities. Although we constructed a few PMD mutants with improved activity toward MVAP, more concerted efforts to engineer PMD promiscuity or identify homologous enzymes should yield additional increases in isopentenol yield and productivity. With further engineering, these bypass pathways will provide valuable platforms for the energetically-favored production of isopentenol, isoprene, and related C_5 compounds.

Acknowledgements

We thank Dr. Miziorko at University of Missouri-Kansas City for providing a plasmid containing the PMD_{se} gene and Dr. Konda at JBEI for discussion on techno-economic impact of this work. This work was part of the DOE Joint BioEnergy Institute (http://www.jbei.org) supported by the U.S. Department of Energy, Office of Science, Office of Biological and Environmental Research, through contract DE-AC02-05CH11231 between Lawrence Berkeley National Laboratory and the U.S. Department of Energy. The United States Government retains and the publisher, by accepting the article for publication, acknowledges that the United States Government retains a non-exclusive, paid-up, irrevocable, world-wide license to publish or reproduce the published form of this manuscript, or allow others to do so, for United States Government purposes.

References

[1] H.H. Chou, J.D. Keasling, Synthetic pathway for production of five-carbon alcohols from isopentenyl diphosphate., Appl. Environ. Microbiol. 78 (2012) 7849–7855. doi:10.1128/AEM.01175-12.

[2] P.P. Peralta-Yahya, F. Zhang, S.B. del Cardayre, J.D. Keasling, Microbial engineering for the production of advanced biofuels., Nature. 488 (2012) 320–328. doi:10.1038/nature11478.

[3] M.R. Connor, J.C. Liao, Engineering of an *Escherichia coli* strain for the production of 3-methyl-1-butanol, Appl. Environ. Microbiol. 74 (2008) 5769–5775. doi:10.1128/AEM.00468-08.

[4] M.R. Connor, A.F. Cann, J.C. Liao, 3-Methyl-1-butanol production in *Escherichia coli*: Random mutagenesis and two-phase fermentation., Appl. Microbiol. Biotechnol. 86 (2010) 1155–1164. doi:10.1007/s00253-009-2401-1.

[5] S.T. Withers, S.S. Gottlieb, B. Lieu, J.D. Newman, J.D. Keasling, Identification of isopentenol biosynthetic genes from *Bacillus subtilis* by a screening method based on isoprenoid precursor toxicity., Appl. Environ. Microbiol. 73 (2007) 6277–6283. doi:10.1128/AEM.00861-07.

[6] K.W. George, A. Chen, A. Jain, T.S. Batth, E. Baidoo, G. Wang, et al., Correlation analysis of targeted proteins and metabolites to assess and engineer microbial isopentenol production, Biotechnol. Bioeng. 111 (2014) 1648–1658. doi:10.1002/bit.25226.

[7] Y. Zheng, Q. Liu, L. Li, W. Qin, J. Yang, H. Zhang, et al., Metabolic engineering of *Escherichia coli* for high-specificity production of isoprenol and prenol as next generation of biofuels., Biotechnol. Biofuels. 6 (2013) 57. doi:10.1186/1754-6834-6-57.

[8] H. Liu, Y. Sun, K.R.M. Ramos, G.M. Nisola, K.N.G. Valdehuesa, W.K. Lee, et al., Combination of entner-doudoroff pathway with MEP increases isoprene production in engineered *Escherichia coli*., PLoS One. 8 (2013) e83290. doi:10.1371/journal.pone.0083290.

[9] K.W. George, M.G. Thompson, A. Kang, E. Baidoo, G. Wang, L.J.G. Chan, et al., Metabolic engineering for the high-yield production of isoprenoid-based C5 alcohols in *E. coli*, Sci. Rep. 5 (2015). doi:10.1038/srep11128.

[10] B.F. Pfleger, D.J. Pitera, C.D. Smolke, J.D. Keasling, Combinatorial engineering of intergenic regions in operons tunes expression of multiple genes., Nat. Biotechnol. 24 (2006) 1027–1032. doi:10.1038/nbt1226.

[11] J.R. Anthony, L.C. Anthony, F. Nowroozi, G. Kwon, J.D. Newman, J.D. Keasling, Optimization of the mevalonate-based isoprenoid biosynthetic pathway in *Escherichia coli* for production of the anti-malarial drug precursor amorpha-4,11-diene, Metab Eng. 11 (2009) 13–19. doi:10.1016/j.ymben.2008.07.007.

[12] J.E. Dueber, G.C. Wu, G.R. Malmirchegini, T.S. Moon, C.J. Petzold, A.V. Ullal, et al., Synthetic protein scaffolds provide modular control over metabolic flux., Nat. Biotechnol. 27 (2009) 753–759. doi:10.1038/nbt.1557.

[13] A.M. Redding-Johanson, T.S. Batth, R. Chan, R. Krupa, H.L. Szmidt, P.D. Adams, et al., Targeted proteomics for metabolic pathway optimization:

Application to terpene production., Metab. Eng. 13 (2011) 194–203. doi:10.1016/j.ymben.2010.12.005.

[14] R.H. Dahl, F. Zhang, J. Alonso-Gutierrez, E. Baidoo, T.S. Batth, A.M. Redding-Johanson, et al., Engineering dynamic pathway regulation using stress-response promoters., Nat. Biotechnol. 31 (2013) 1039–1046. doi:10.1038/nbt.2689.

[15] F. Zhu, X. Zhong, M. Hu, L. Lu, Z. Deng, T. Liu, In vitro reconstitution of mevalonate pathway and targeted engineering of farnesene overproduction in *Escherichia coli*, Biotechnol. Bioeng. 111 (2014) 1396–1405. doi:10.1002/bit.25198.

[16] V.J.J. Martin, D.J. Pitera, S.T. Withers, J.D. Newman, J.D. Keasling, Engineering a mevalonate pathway in *Escherichia coli* for production of terpenoids., Nat. Biotechnol. 21 (2003) 796–802. doi:10.1038/nbt833.

[17] D.J. Pitera, C.J. Paddon, J.D. Newman, J.D. Keasling, Balancing a heterologous mevalonate pathway for improved isoprenoid production in *Escherichia coli*, Metab. Eng. 9 (2007) 193–207. doi:10.1016/j.ymben.2006.11.002.

[18] R. Hengge, The two-component network and the general stress sigma factor RpoS (sigma S) in *Escherichia coli*., Adv. Exp. Med. Biol. 631 (2008) 40–53. doi:10.1007/978-0-387-78885-2_4.

[19] Y. Sun, T. Fukamachi, H. Saito, H. Kobayashi, ATP requirement for acidic resistance in *Escherichia coli*., J. Bacteriol. 193 (2011) 3072–3077. doi:10.1128/JB.00091-11.

[20] K.J. Adolfsen, M.P. Brynildsen, Futile cycling increases sensitivity toward oxidative stress in *Escherichia coli*, Metab. Eng. 29 (2015) 26–35. doi:10.1016/j.ymben.2015.02.006.

[21] B.E. Cohen, Functional linkage between genes that regulate osmotic stress responses and multidrug resistance transporters: challenges and opportunities for antibiotic discovery., Antimicrob. Agents Chemother. 58 (2014) 640–646. doi:10.1128/AAC.02095-13.

[22] S.M. Ma, D.E. Garcia, A.M. Redding-Johanson, G.D. Friedland, R. Chan, T.S. Batth, et al., Optimization of a heterologous mevalonate pathway through the use of variant HMG-CoA reductases., Metab. Eng. 13 (2011) 588–597. doi:10.1016/j.ymben.2011.07.001.

[23] M.L. Barta, W.J. McWhorter, H.M. Miziorko, B. Geisbrecht, Structural basis for nucleotide binding and reaction catalysis in mevalonate diphosphate decarboxylase, Biochemistry. 51 (2012) 5611–5621. doi:10.1021/bi300591x.

[24] J.C. Vannice, D.A. Skaff, A. Keightley, J.K. Addo, G.J. Wyckoff, H.M. Miziorko, Identification in *Haloferax volcanii* of phosphomevalonate decarboxylase and isopentenyl phosphate kinase as catalysts of the terminal enzyme reactions in an archaeal alternate mevalonate pathway, J. Bacteriol. 196 (2014) 1055–1063. doi:10.1128/JB.01230-13.

[25] T. Baba, T. Ara, M. Hasegawa, Y. Takai, Y. Okumura, M. Baba, et al., Construction of *Escherichia coli* K-12 in-frame, single-gene knockout mutants: the Keio collection., Mol. Syst. Biol. 2 (2006) 2006.0008. doi:10.1038/msb4100050.

[26] T.S. Lee, R.A. Krupa, F. Zhang, M. Hajimorad, W.J. Holtz, N. Prasad, et al.,

BglBrick vectors and datasheets: A synthetic biology platform for gene expression., J. Biol. Eng. 5 (2011) 12. doi:10.1186/1754-1611-5-12.

[27] J. Degenhardt, T.G. Köllner, J. Gershenzon, Monoterpene and sesquiterpene synthases and the origin of terpene skeletal diversity in plants., Phytochemistry. 70 (2009) 1621–1637. doi:10.1016/j.phytochem.2009.07.030.

[28] J. Alonso-Gutierrez, R. Chan, T.S. Batth, P.D. Adams, J.D. Keasling, C.J. Petzold, et al., Metabolic engineering of *Escherichia coli* for limonene and perillyl alcohol production, Metab. Eng. 19 (2013) 33–41. doi:10.1016/j.ymben.2013.05.004.

[29] E.M. Kim, J.H. Eom, Y. Um, Y. Kim, H.M. Woo, Microbial Synthesis of Myrcene by Metabolically Engineered *Escherichia coli*., J. Agric. Food Chem. 63 (2015) 4606–4612. doi:10.1021/acs.jafc.5b01334.

[30] C. Wang, S.H. Yoon, A.A. Shah, Y.R. Chung, J.Y. Kim, E.S. Choi, et al., Farnesol production from *Escherichia coli* by harnessing the exogenous mevalonate pathway., Biotechnol. Bioeng. 107 (2010) 421–9. doi:10.1002/bit.22831.

[31] D.S. Gogerty, T.A. Bobik, Formation of isobutene from 3-hydroxy-3-methylbutyrate by diphosphomevalonate decarboxylase., Appl. Environ. Microbiol. 76 (2010) 8004–8010. doi:10.1128/AEM.01917-10.

[32] D. Krepkiy, H.M. Miziorko, Identification of active site residues in mevalonate diphosphate decarboxylase: implications for a family of phosphotransferases., Protein Sci. 13 (2004) 1875–1881. doi:10.1110/ps.04725204.

[33] S. Wagner, M.M. Klepsch, S. Schlegel, A. Appel, R. Draheim, M. Tarry, et al.,

Tuning *Escherichia coli* for membrane protein overexpression., Proc. Natl. Acad. Sci. USA. 105 (2008) 14371–14376. doi:10.1073/pnas.0804090105.

[34] J.B. Bonanno, C. Edo, N. Eswar, U. Pieper, M.J. Romanowski, V. Ilyin, et al., Structural genomics of enzymes involved in sterol/isoprenoid biosynthesis., Proc. Natl. Acad. Sci. USA. 98 (2001) 12896–12901. doi:10.1073/pnas.181466998.

[35] D.S. Clark, H.W. Blanch, Biochemical Engineering, Second Edition, CRC Press, 1997. https://books.google.com/books?id=ST_p2AOApZsC&pgis=1 (accessed August 12, 2015).

Figure legends

Fig. 1. Original and two modified mevalonate pathways for isopentenol production. The original mevalonate pathway (pathway O) produces isopentenyl diphosphate (IPP), which is dephosphorylated by NudB, as an intermediate. Two modified pathways were proposed in this study: direct decarboxylation of mevalonate (pathway I) or decarboxylation of mevalonate diphosphate (pathway II) followed by de-phosphorylation of isopentenyl monophosphate (IP). Numbers of ATP and enzymes required for each pathway are summarized in the table. Ac-CoA, acetyl-CoA; AAc-CoA, acetoacetyl-CoA; HMG-CoA, 3-hydroxy-3-methyl-glutaryl-CoA; PMK, phosphomevalonate kinase; PMD, phosphomevalonate decarboxylase)

Fig. 2. GC/MS chromatogram (left) and mass spectra (right) of ethyl acetate-extracted metabolites detected from (A) control strain with three genes (ARK3a; *atoB*, *HMGS*, *HMGR*) and (B) engineered strains with four genes (ARK3b; *atoB*, *HMGS*, *HMGR* and PMD_{sc}). The mass spectrum of the peak that eluted at 9.49 min detected in ARK3b (B) is very similar to that of the isopentenol standard (C), and is not present in the ethyl acetate blank (D). Arrows indicate masses of the peak at retention time of 9.49 min detected from both standard (C) and the engineered strain (B; ARK3b).

Fig. 3. Hydrolysis of IP and IPP by purified NudB or *E. coli* cell lysates. (A) IP hydrolysis. IP was hydrolyzed to isopentenol by *E. coli* cell lysates while isopentenol was not detected (*) from other two reactions with or without purified NudB. (B) Profile of IP and IPP concentrations in *in vitro* hydrolysis reactions of IPP by purified NudB.

Fig. 4. Identification of endogenous phosphatases for IP. (A) Isopentenol concentration (μM) in the cell lysates of monophosphatase mutants. A total of 36 mutants (diamonds)—including *ΔagpA* (solid circle), *ΔyqaB* (solid triangle), *ΔaphA* (solid square) mutants and wild type BW25113 (open circle)—were screened. The grey line represents the average (251.9 μM) of isopentenol concentrations detected from all mutants. (B) Isopentenol converted from 1 mM IP by cell lysates of wild type (BW25113, empty circle), *ΔagpA* (circle), *ΔyqaB* (triangle) and *ΔaphA* (square) mutants. (C) Isopentenol converted from 500 μM IP by cell lysates of wild type (solid lines) or each mutant (dotted lines) with overexpression of the corresponding gene: *agpA* (circle), *yqaB* (triangle) and *aphA* (square).

Fig. 5. Effect of *aphA* expression on isopentenol production in pathway II. Isopentenol from pathway II with (dark grey bar) or without *aphA* expression (white bar). Optical density of cell cultures at 600 nm (OD_{600}) for pathway II with (solid circle) or without *aphA* expression (open circle)

Fig. 6. Effect of mutations on isopentenol production with IPP-bypass pathway II. (A) location of R74 and I145 in PMD_{sc}. Blue meshes are essential residues for catalysis and substrate binding, and pink meshes are residues selected for mutagenesis. Electrostatic interactions were not clearly found between substrates and these residues and the distance between phosphate group of the substrate analog (6-fluoromevalonate 5-diphosphate (FMVAPP)) and R74 or I145 residue were 12.5 Å or 15.0 Å, respectively. (B) Curve fittings and kinetics of PMD_{sc} wild type and four mutants (K22M, R74H, I145F and

T209D). (C) Isopentenol production from strains with pathway II containing different PMD mutants including wild type (WT, black square), R74H (open circle), I145F (grey circle) and R74H/I145F double mutants (black circle).

Fig. 7. Effect of different "top" portions on isopentenol production in *E. coli* with pathway O or with pathway II. Four different "top" portions have different HMGS and HMGR sequences, which are original sequences from. *S. cerevisiae* (MevTo), codon-optimized sequences of *S. cerevisiae* (MevTco), sequences from *S. aureus* (MTSA) and sequences from *D. acidovorans* (MTDA). Isopentenol production was measured at 24 hours (white dotted bar) and at 48 hours (grey bars).

Fig. 8. IPP toxicity in Pathway O. (A) Growth of four strains containing Pathway O without (black, square) or with expression of additional MK (white square); Pathway II without (black, circle) or with expression of additional MK (white circle). (B) Isopentenol production from four strains containing Pathway O without or with expression of additional MK; Pathway II without or with expression of additional MK.

Fig. 9. Effect of reduced aeration conditions on isopentenol production in *E. coli*. (A) Isopentenol titers (per OD_{600}) of two strains with pathway O or with pathway II under higher (200 rpm) or lower (30 rpm) aeration conditions. (B) Relative isopentenol titers (total) of two pathways under lower aeration conditions (30 rpm) compared to those under higher aeration conditions (200 rpm).

772 **Table 1** List of strains and plasmids used in this study

Strains	Description	Reference
ΔaphA	*E. coli* K12 BW25113 *ΔaphA*	Keio Collection [25]
Δagp	*E. coli* K12 BW25113 *Δagp*	Keio Collection [25]
ΔyqaB	*E. coli* K12 BW25113 *ΔyqaB*	Keio Collection [25]
ARK1a	JBEI-12056 + JBEI-9348	This study
ARK1b	JBEI-6824 + JBEI-9348	This study
ARK1c	JBEI-6831 + JBEI-9348	This study
ARK1d	JBEI-7575 + JBEI-9348	This study
ARK1e	JBEI-6818 + JBEI-6833	This study
ARK1f	JBEI-6818 + JBEI-6834	This study
ARK2a	JBEI-9310 + JBEI-9314	This study
ARK2b	JBEI-9309 + JBEI-9314	This study
ARK2c	JBEI-9312 + JBEI-9314	This study
ARK2d	JBEI-9311 + JBEI-9314	This study
ARK2e	JBEI-12051 + JBEI-9314	This study
ARK2f	JBEI-12051 + JBEI-12064	This study
ARK2aa	JBEI-12050 + JBEI-9314	This study
$ARK2a_{M1}$	JBEI-9310 + JBEI-12060	This study
$ARK2a_{M2}$	JBEI-9310 + JBEI-12061	This study
$ARK2a_{M3}$	JBEI-9310 + JBEI-12062	This study
ARK3a	JBEI-3100 + JBEI-12229	This study
ARK3b	JBEI-3100 + JBEI-3277	This study
ARK4	JBEI-9310 + JBEI-12054	This study
ARK5	JBEI-9310 + JBEI-12059	This study

Plasmids	Description	Reference
JBEI-6818	pBbA5c-MevTo-MKco-PMKco	[6]
JBEI-6824	pBbA5c-MevTco-BBa1002-pTrc-MKco-PMKco	[6]
JBEI-6831	pBbA5c-MTSA-BBa1002-pTrc-MKco-PMKco	[6]
JBEI-6833	pTrc99a-NudB-PMDsc	[6]
JBEI-6834	pTrc99a-NudB-PMDsc-Mkco	[6]
JBEI-7575	pBbA5c-MTDA-BBa1002-pTrc-MKco-PMKco	Gift from Eunmi Kim
JBEI-9309	pBbA5c-MevTco-BBa1002-pTrc-MKco	This study
JBEI-9310	pBbA5c-MevTo-BBa1002-pTrc-MKco	This study
JBEI-9311	pBbA5c-MTDA-BBa1002-pTrc-MKco	This study
JBEI-9312	pBbA5c-MTSA-BBa1002-pTrc-MKco	This study
JBEI-9314	pTrc99a-PMDsc	This study
JBEI-9348	pTrc99a-PMDsc-NudB	This study
JBEI-12050	pBbA5c-MevTo-BBa1002-pTrc-MKco-aphA	This study
JBEI-12051	pBbA5c-MevTo-MKco	This study

JBEI-12052	pSKB3-PMDsc	This study
JBEI-12053	pSKB3-PMDsc_K22M	This study
JBEI-12054	pTrc99a-PMDse	This study
JBEI-12055	pSKB3-PMDsc_T209D	This study
JBEI-12056	pBbA5c-MevTo-BBa1002-pTrc-MKco-PMKco	This study
JBEI-12057	pSKB3-PMDsc_R74H	This study
JBEI-12058	pSKB3-PMDsc_I145F	This study
JBEI-12059	pTrc99a-PMDhv	This study
JBEI-12060	pTrc99a-PMDsc_R74H	This study
JBEI-12061	pTrc99a-PMDsc_I145F	This study
JBEI-12062	pTrc99a-PMDsc_R74H/I145F	This study
JBEI-12064	pTrc99a-PMDsc-MKco	This study
JBEI-12229	pE1a-PMDsc	This study

773

774

Table 2. Kinetic parameters of PMD wild type, PMD_{sc} mutants, PMD_{se}, PMD_{hv} from other literatures.

Name		K_m (mM)	k_{cat} (s^{-1})	k_{cat}/K_m (s^{-1} M^{-1})	% of WT	Substrate	Reference
PMD_{sc}	WT	0.99	0.14	1.4×10^2	100%	MVAP	This study
	R74H	0.77	0.23	3.0×10^2	220%		
	K22M	2.47	0.09	3.5×10^1	25%		
	T209D	0.99	0.13	1.3×10^2	98%		
	I145F	1.36	0.28	2.0×10^2	147%		
PMD_{hv}		0.159	3.5	2.2×10^4		MVAP	[24]
PMD_{se}		0.009	5.9	6.5×10^5		MVAPP	[23]
PMD_{sc}		0.123	5.4	4.0×10^4		MVAPP	[32]

Figure1
Click here to download high resolution image

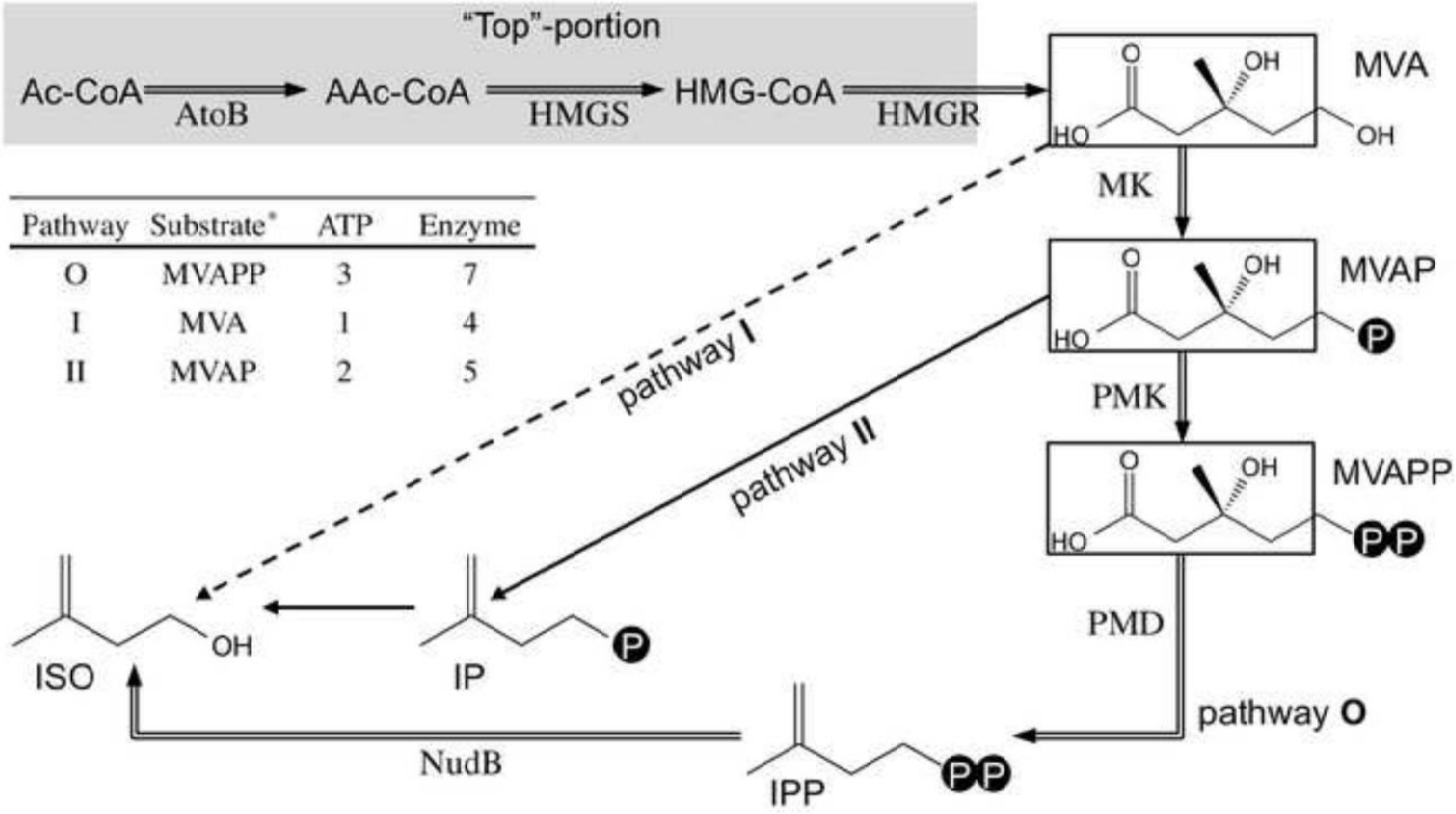

Pathway	Substrate*	ATP	Enzyme
O	MVAPP	3	7
I	MVA	1	4
II	MVAP	2	5

Figure2

Click here to download high resolution image

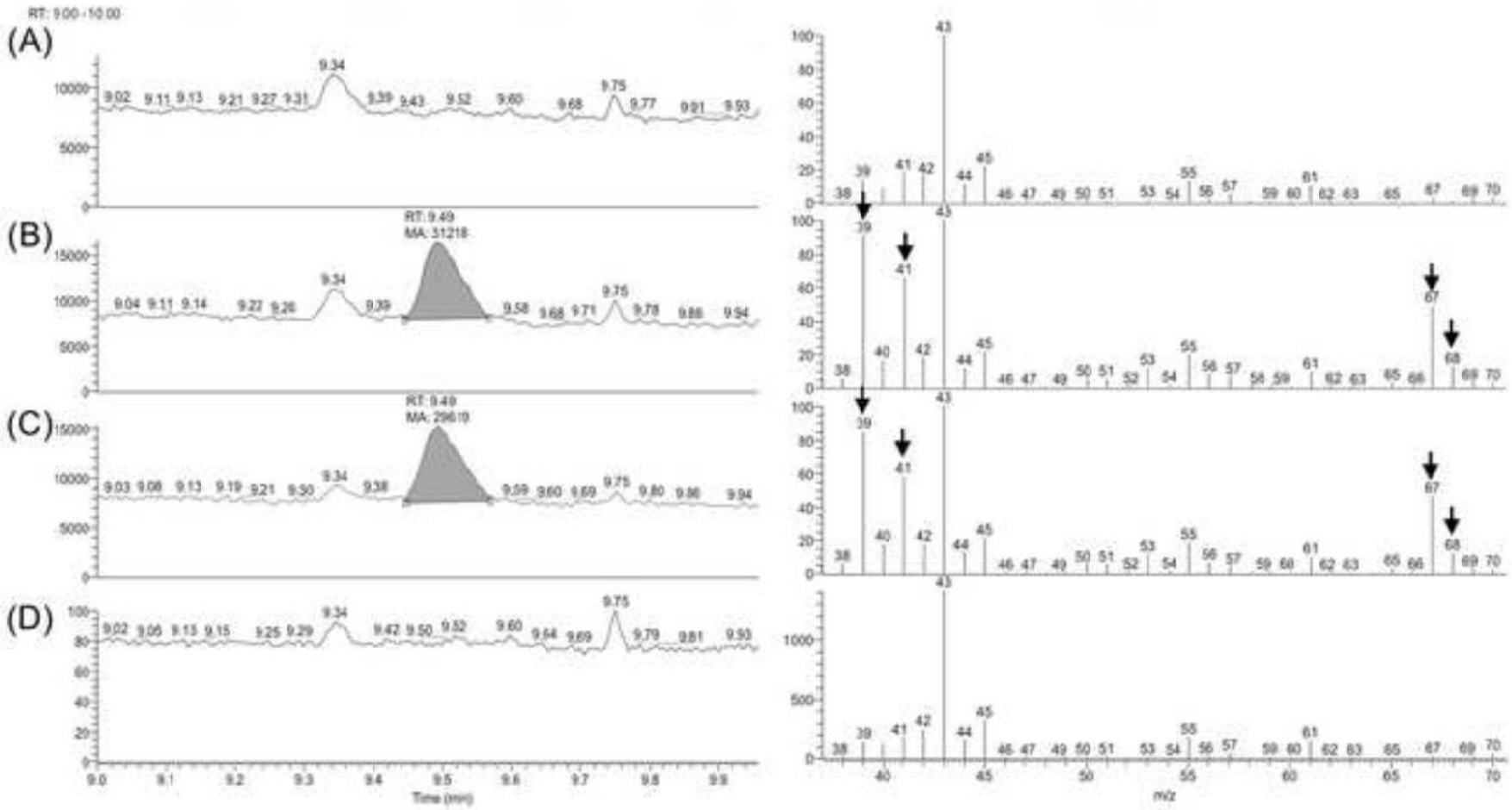

Figure3
Click here to download high resolution image

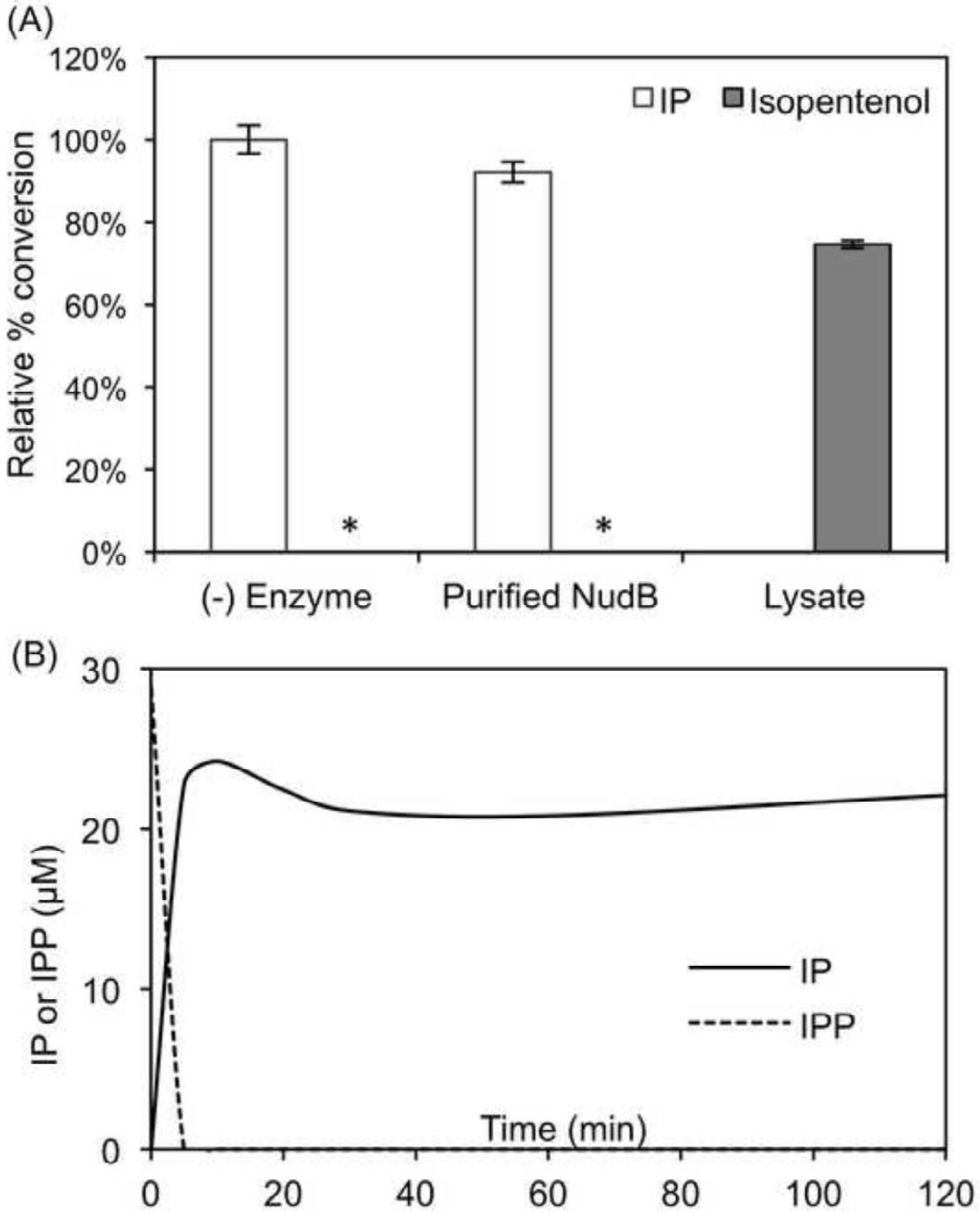

Figure4

Click here to download high resolution image

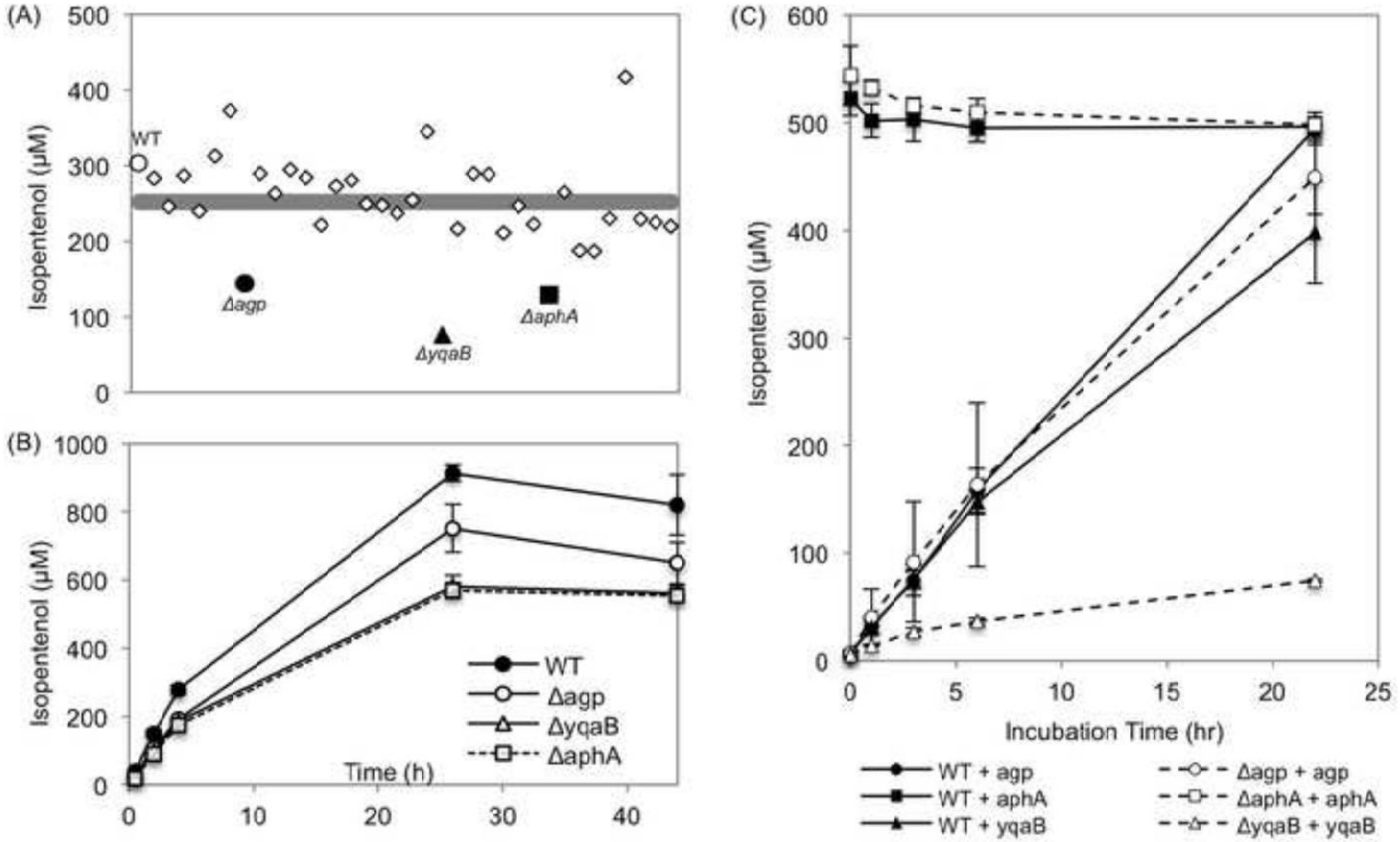

Figure5
Click here to download high resolution image

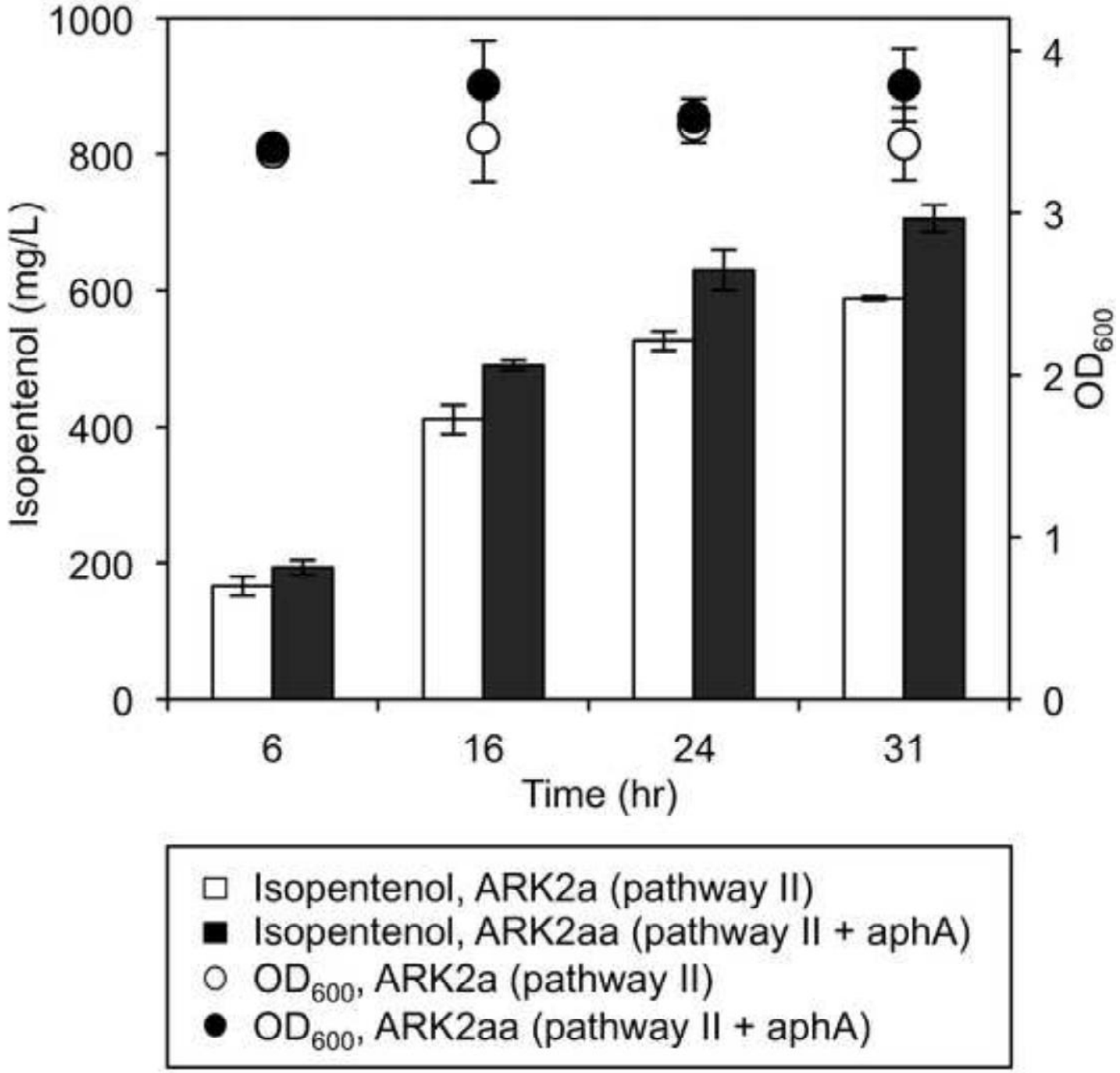

Figure6

Click here to download high resolution image

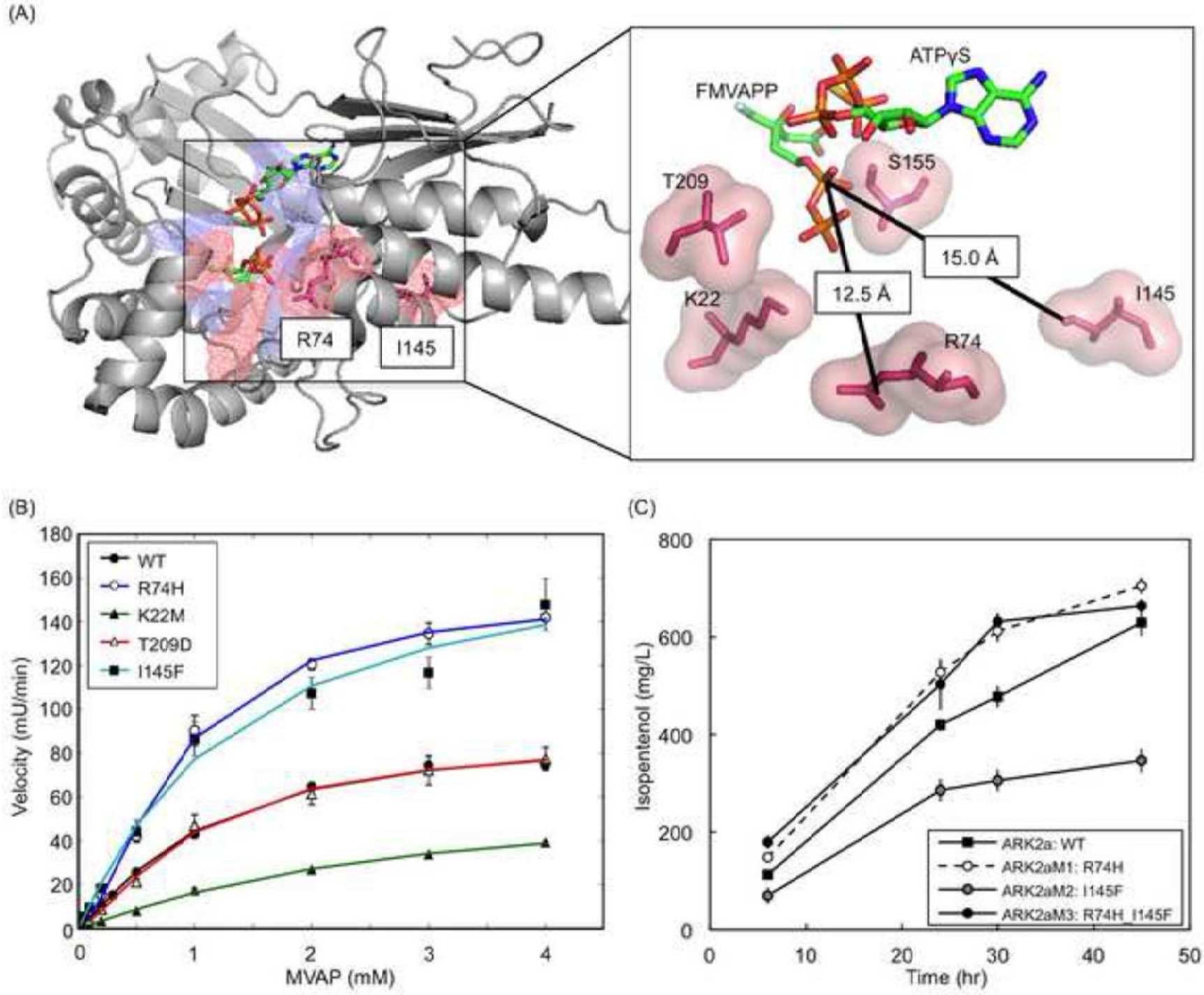

Figure7
Click here to download high resolution image

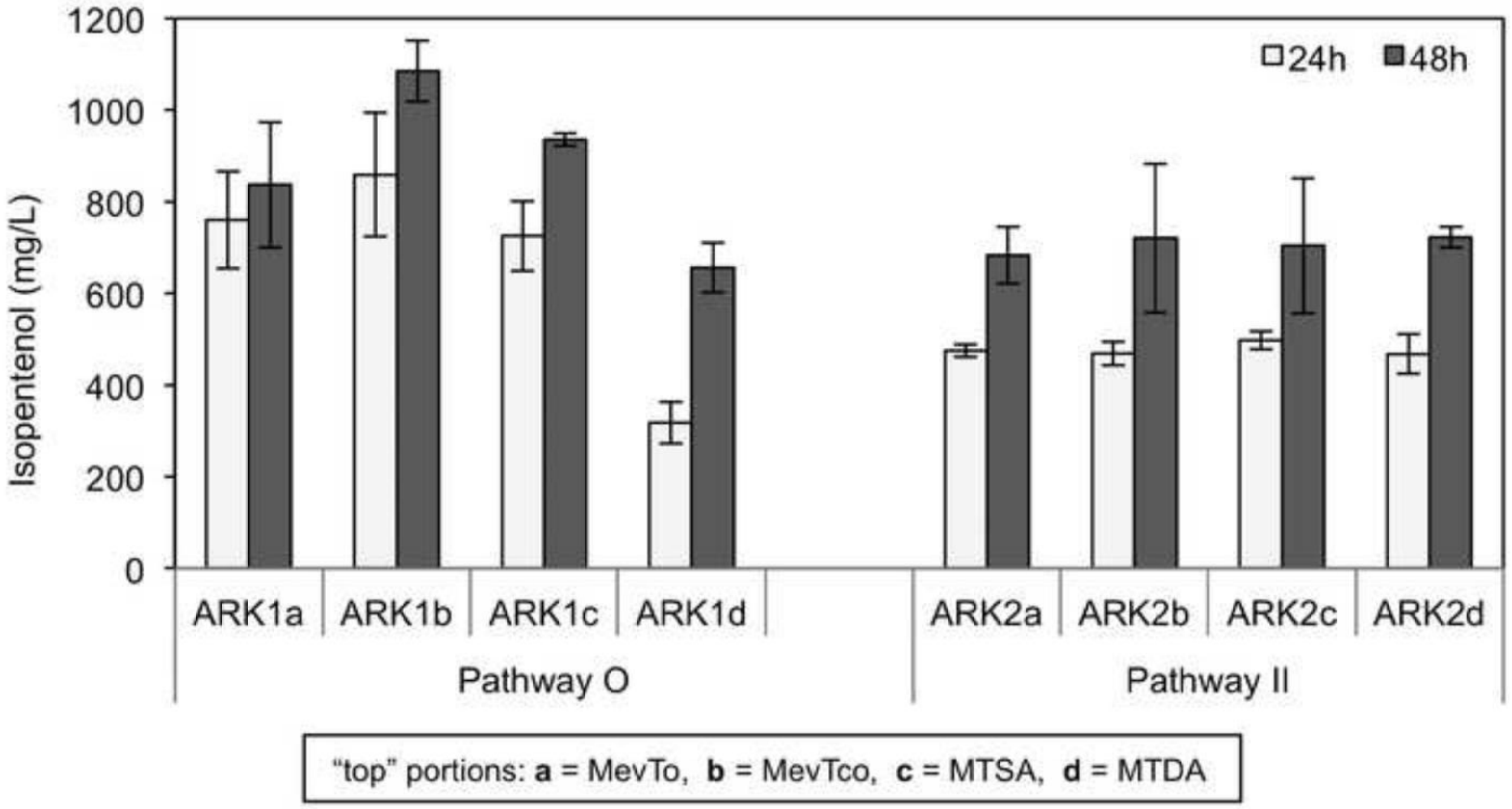

Figure8
Click here to download high resolution image

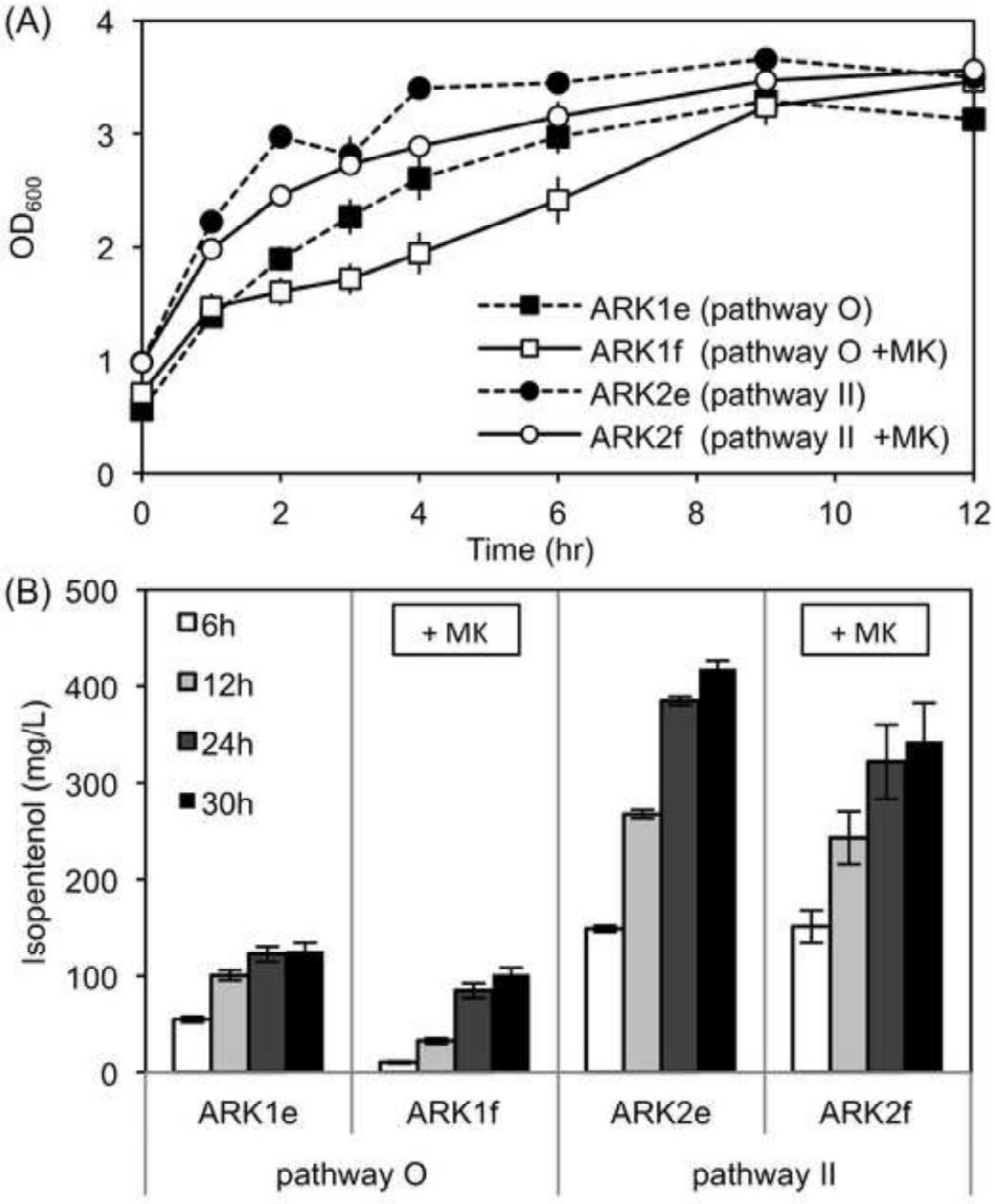

Figure9

Click here to download high resolution image

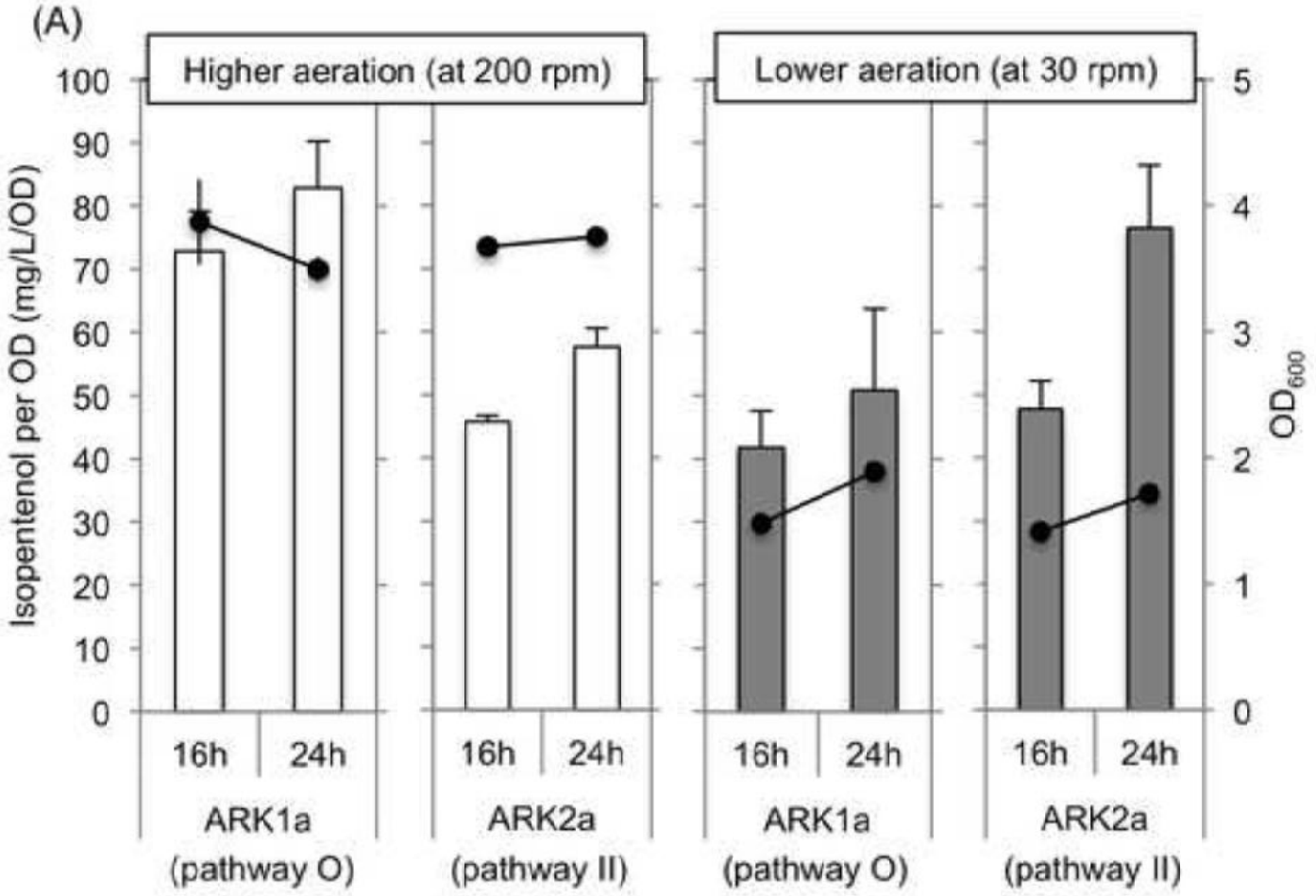

(B)

Isopentenol titers at 30 rpm / Isopentenol titers at 200 rpm X 100	16h	24h
ARK1a (pathway O)	22%	33%
ARK2a (pathway II)	40%	60%

Supplementary Material

Isopentenyl diphosphate (IPP)-bypass mevalonate pathways for isopentenol production

Aram Kang, Kevin W. George, George Wang, Edward Baidoo, Jay D. Keasling, Taek Soon Lee*

Fig. S1. A diagram of PMD_{sc} active sites with two substrates, MVAPP and ATP: (A) Catalytically important residues (R158 and D302) near the mevalonate-derived carbon backbone, and (B) residues (S208 and S120) that interact with phosphate groups of two substrates (MVAPP and ATP).

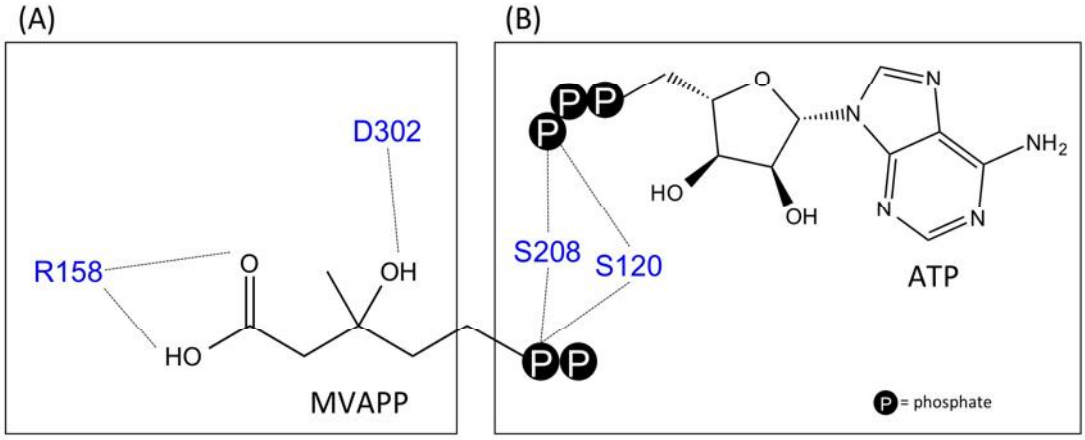

Fig. S2. Kinetics of wild type PMD toward MVAP: k_{cat} and K_m were determined as 0.14 s^{-1} and 0.99 mM, respectively. Each data points are average of duplicates, and the curve was fit by Hill equation.

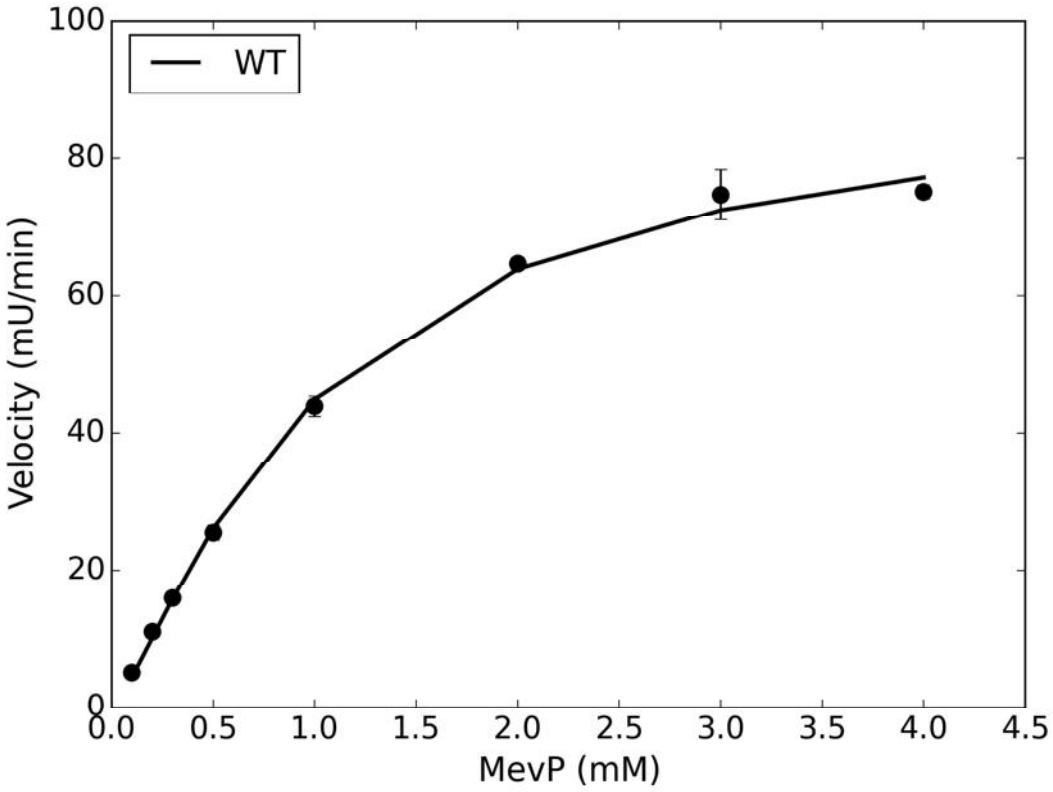

Fig. S3. (A) Hydrolysis of DMAPP by NudB and (B) hydrolysis of IPP by NudF

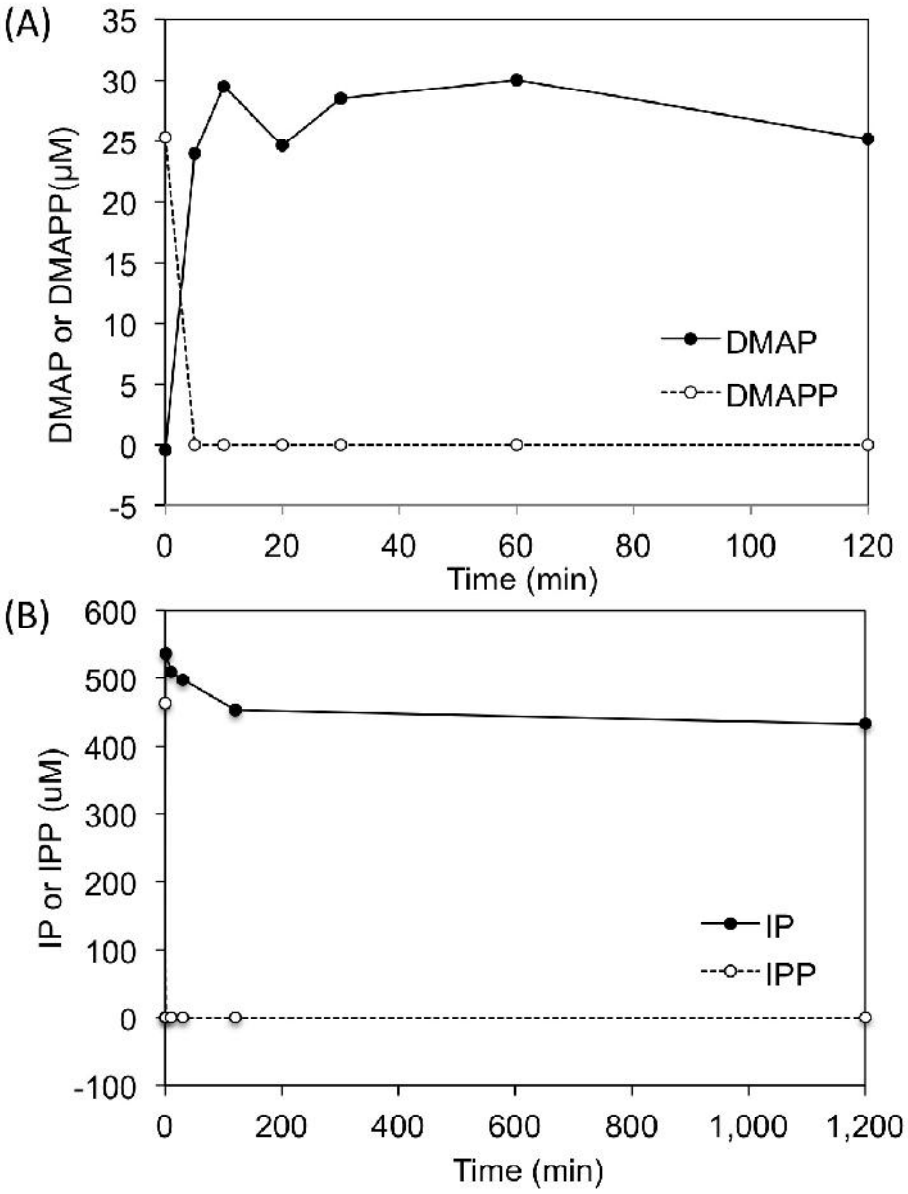

Fig. S4. (A) Structural alignment of PMD_{sc} (grey) and PMD_{se} (cyan). (B) BLAST alignment of two PMD sequences, PMD from *S. cerevisiae* (PMD_{sc}, sequence 1) and PMD from *S. epidermis* (PMD_{se}, sequence 2): Conserved residues suggested by structure-based alignment of prokaryotic and eukaryotic PMD sequences in a study (Barta et al., 2012). More strictly conserved residues were highlighted with red and similarly conserved residues with blue. Stars below sequences denote residues that interact with ATP (black) or MVAPP (red). R193 and T209 were indicated with a box.

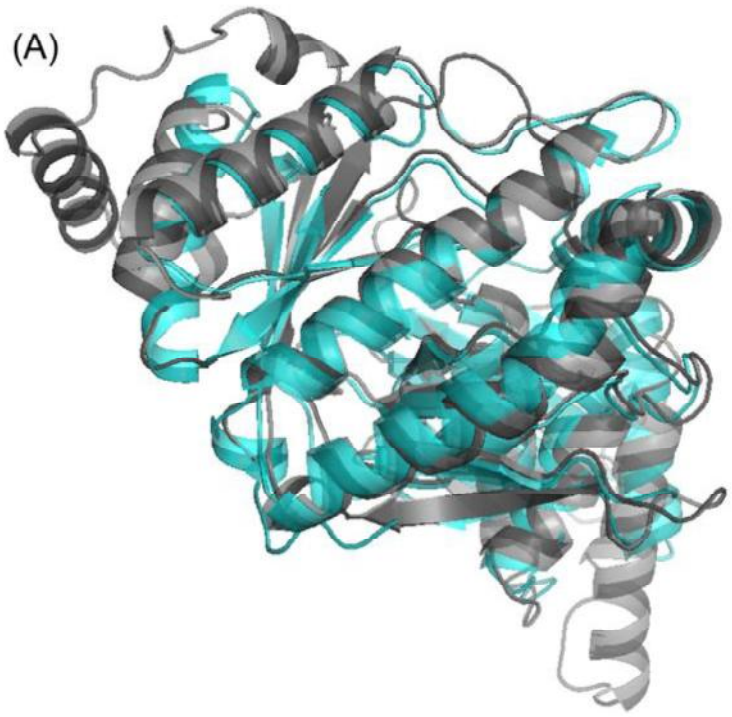

(B)

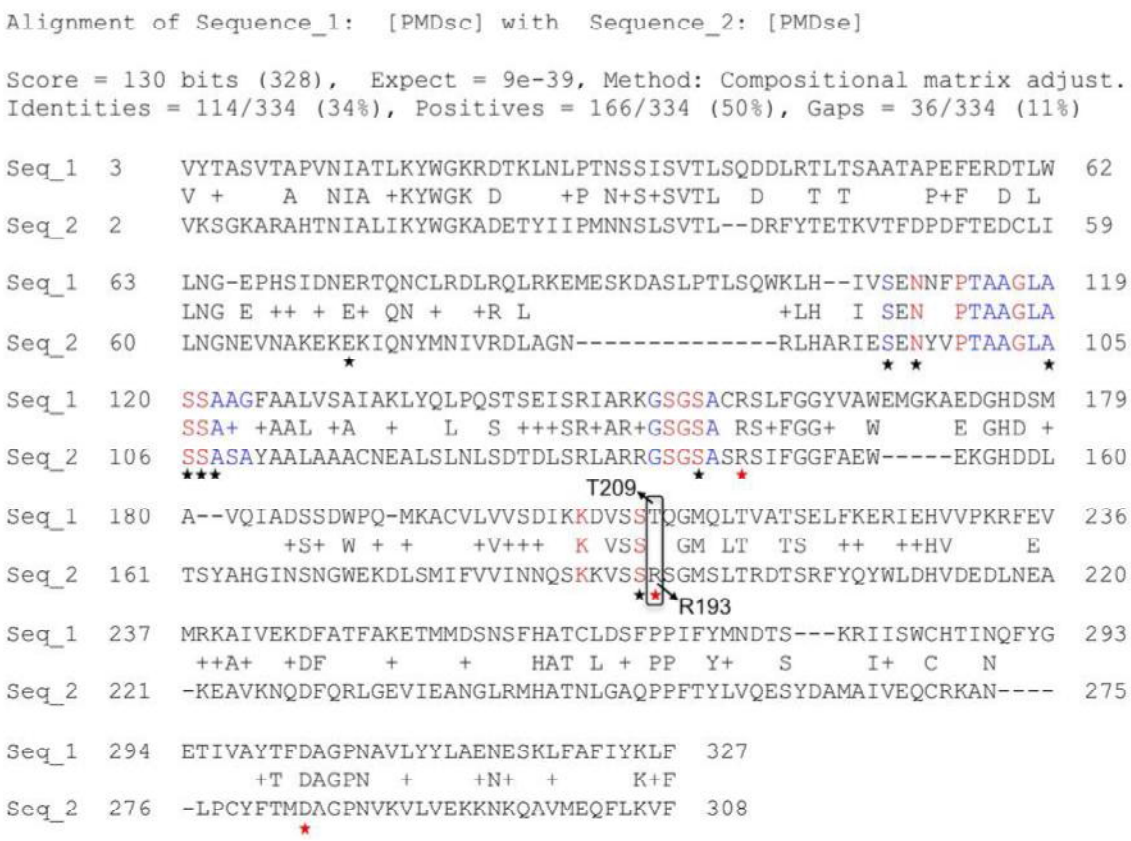
Alignment of Sequence_1: [PMDsc] with Sequence_2: [PMDse]
Score = 130 bits (328), Expect = 9e-39, Method: Compositional matrix adjust.
Identities = 114/334 (34%), Positives = 166/334 (50%), Gaps = 36/334 (11%)
Seq_1 3 VYTASVTAPVNIATLKYWGKRDTKLNLPTNSSISVTLSQDDLRTLTSAATAPEFERDTLW 62
V + A NIA +KYWGK D +P N+S+SVTL D T T P+F D L
Seq_2 2 VKSGKARAHTNIALIKYWGKADETYIIPMNNSLSVTL--DRFYTETKVTFDPDFTEDCLI 59
Seq_1 63 LNG-EPHSIDNERTQNCLRDLRQLRKEMESKDASLPTLSQWKLH--IVSENNFPTAAGLA 119
LNG E ++ + E+ QN + +R L +LH I SEN PTAAGLA
Seq_2 60 LNGNEVNAKEKEKIQNYMNIVRDLAGN--------------RLHARIESENYVPTAAGLA 105
Seq_1 120 SSAAGFAALVSAIAKLYQLPQSTSEISRIARKGSGSACRSLFGGYVAWEMGKAEDGHDSM 179
SSA+ +AAL +A + L S +++SR+AR+GSGSA RS+FGG+ W E GHD +
Seq_2 106 SSASAYAALAAACNEALSLNLSDTDLSRLARRGSGSASRSIFGGFAEW-----EKGHDDL 160
T209
Seq_1 180 A--VQIADSSDWPQ-MKACVLVVSDIKKDVSSTQGMQLTVATSELFKERIEHVVPKRFEV 236
+S+ W + + +V+++ K VSS GM LT TS ++ ++HV E
Seq_2 161 TSYAHGINSNGWEKDLSMIFVVINNQSKKVSSRSGMSLTRDTSRFYQYWLDHVDEDLNEA 220
R193
Seq_1 237 MRKAIVEKDFATFAKETMMDSNSFHATCLDSFPPIFYMNDTS---KRIISWCHTINQFYG 293
++A+ +DF + + HAT L + PP Y+ S I+ C N
Seq_2 221 -KEAVKNQDFQRLGEVIEANGLRMHATNLGAQPPFTYLVQESYDAMAIVEQCRKAN---- 275
Seq_1 294 ETIVAYTFDAGPNAVLYYLAENESKLFAFIYKLF 327
+T DAGPN + +N+ + K+F
Seq_2 276 -LPCYFTMDAGPNVKVLVEKKNKQAVMEQFLKVF 308

50

51

52

Fig. S5. Four residues (K22, S155, S208 and T209) of PMD_{sc} near the β-phosphate ($P_β$) of FMVAPP, an analog of MVAPP, which was used in a crystal structure of PMD_{se} (4DPT): Coordinates of two substrates analogs (FMVAPP and ATPγS) in PMD_{sc} crystal structure were predicted by structural alignment of two PMD sequences (PMD_{sc} and PMD_{se}).

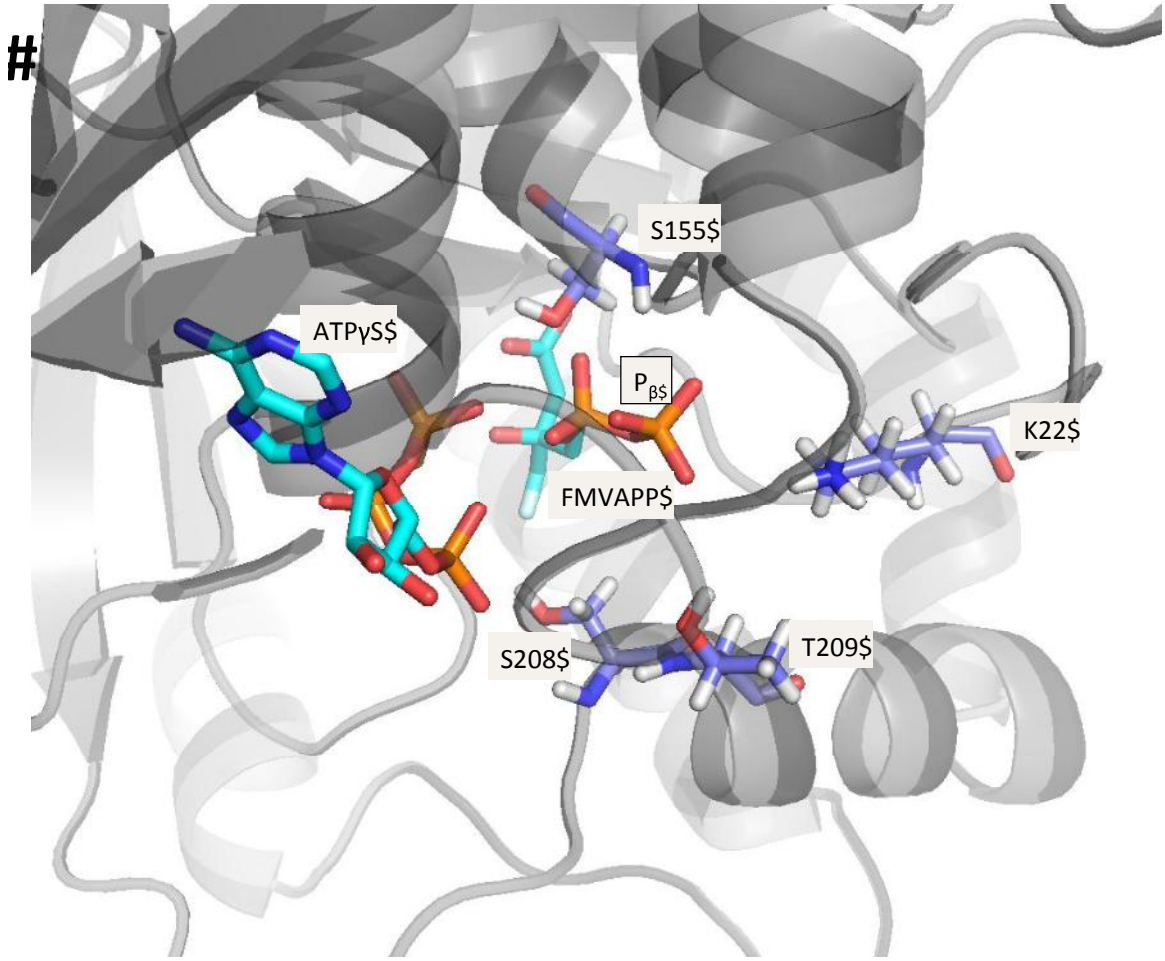

Fig. S6. Quantitation of intracellular metabolites: (A) MVA, (B) MVAP, (C) IPP and (D) IP in the original isopentenol pathway (pathway O) and IPP-bypass pathway II (pathway II) with four different "top" portions (MevTo, MevTco, MTSA and MTDA).

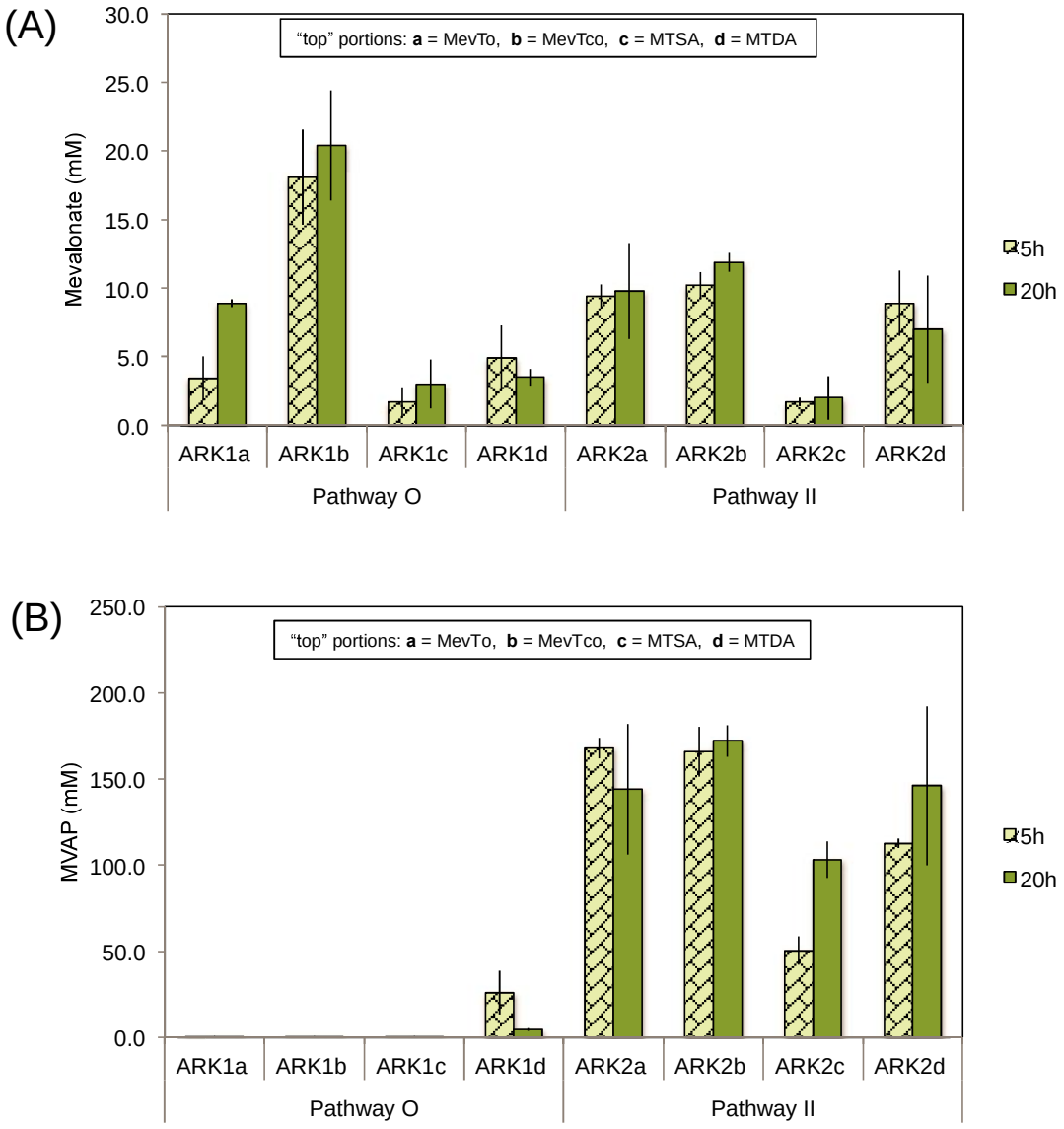

(C)

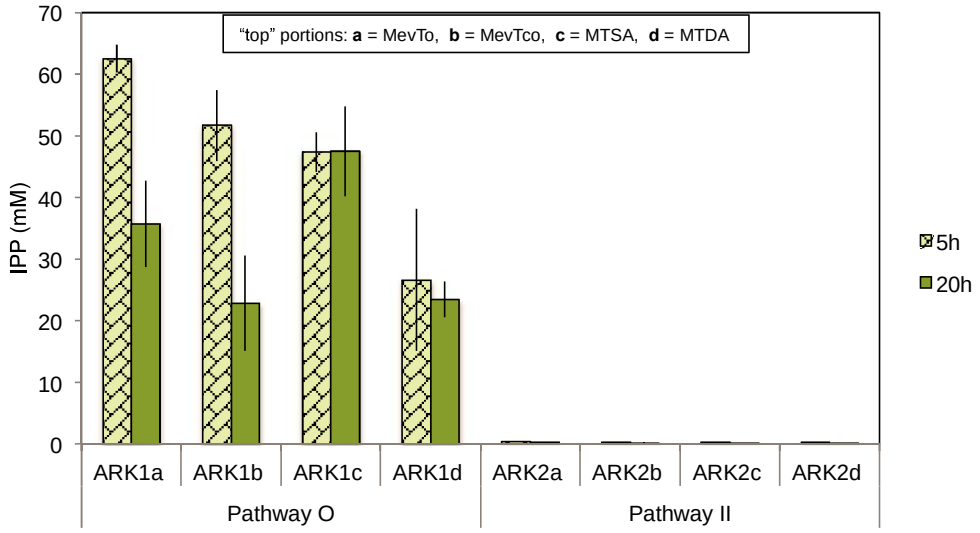
"top" portions: **a** = MevTo, **b** = MevTco, **c** = MTSA, **d** = MTDA
IPP (mM)
70
60
50
40
30
20
10
0
ARK1a
ARK1b
ARK1c
ARK1d
ARK2a
ARK2b
ARK2c
ARK2d
Pathway O
Pathway II
5h
20h

(D)

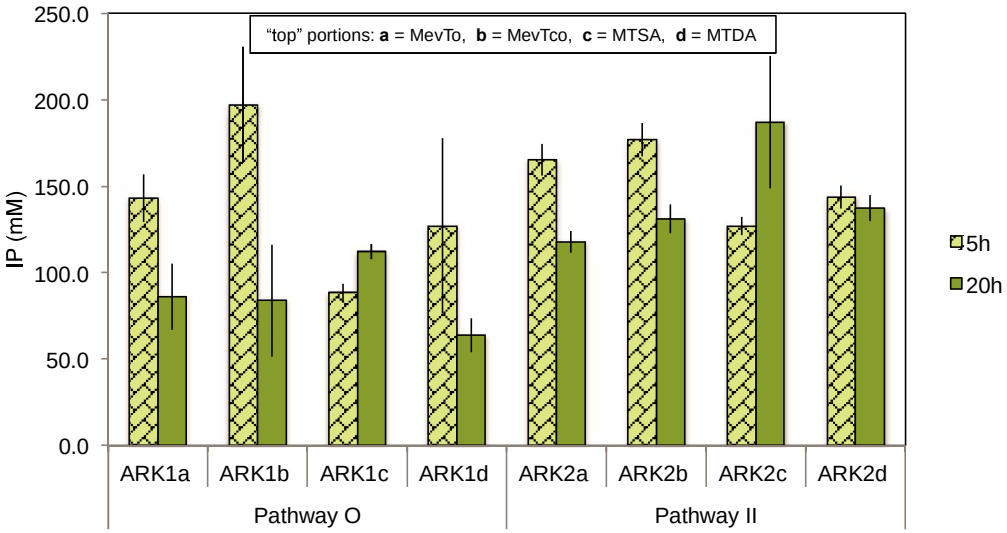
"top" portions: **a** = MevTo, **b** = MevTco, **c** = MTSA, **d** = MTDA
IP (mM)
250.0
200.0
150.0
100.0
50.0
0.0
ARK1a
ARK1b
ARK1c
ARK1d
ARK2a
ARK2b
ARK2c
ARK2d
Pathway O
Pathway II
5h
20h

64
65

Fig. S7. A schematic diagram to show construction of ARK1e, ARK1f, ARK2e and ARK2f for IPP toxicity experiments. All strains harbor two plasmids. The first plasmid containing MevTo and MK is medium copy (p15A origin) plasmid with P_{lacUV5} promoter, and the other plasmid is high copy (ColE1 origin) plasmid with P_{trc} promoter.

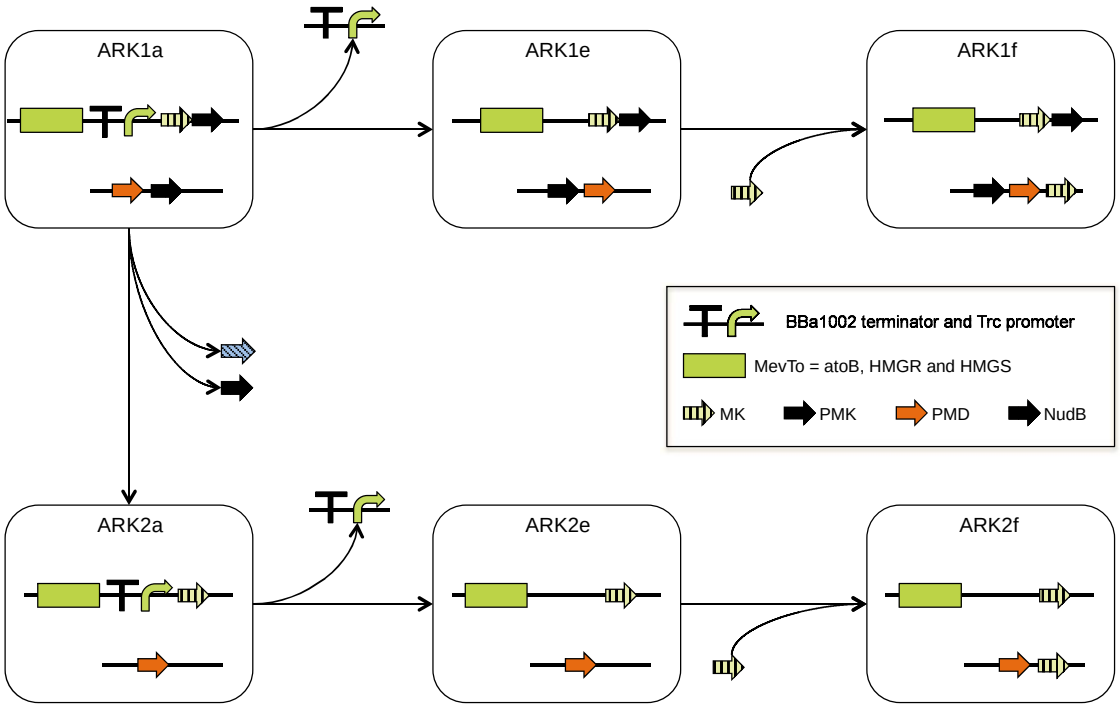

Fig. S8. Isopentenol titers (total) of strains with the original isopentenol pathway (ARK1a; pathway O) or with the IPP-bypass pathway II (ARK2a; pathway II) under two different aeration conditions (High, 200 rpm; Low, 30 rpm)

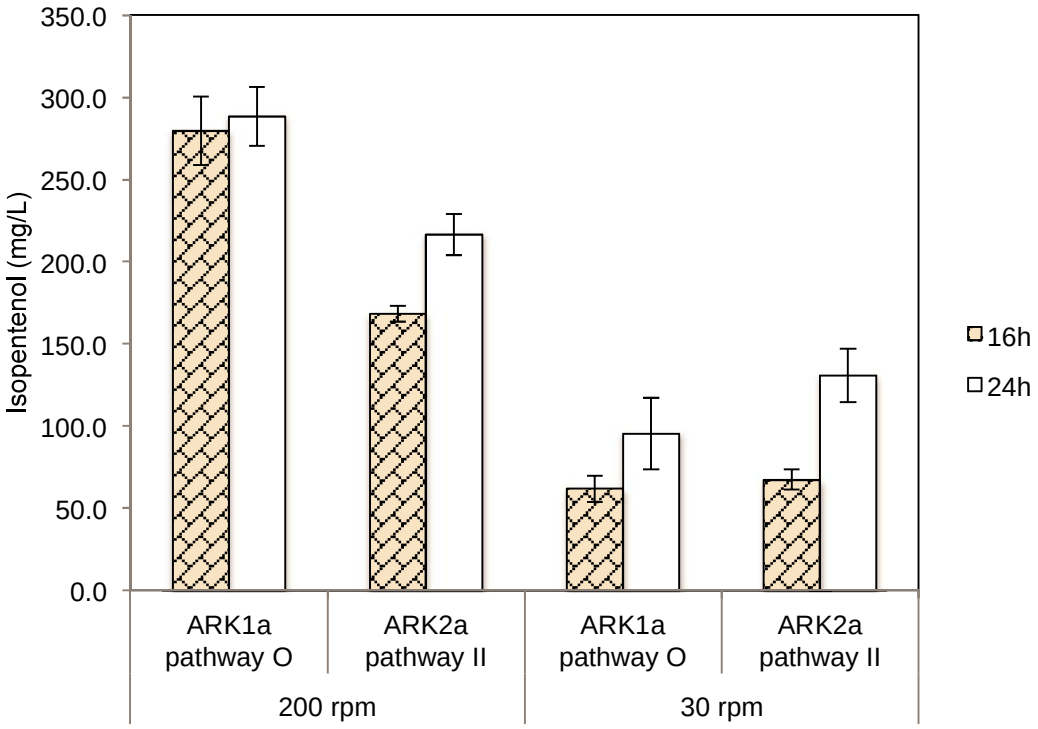

Table S1. List of primers used in this study.

Primers	Sequence
aphA-F-NdeI	GGGCCATATGCGCAAGATCACAC
aphA-R-BamHI	CAGAGGATCCTCAGTATTCTGAATTG
agp-F-NdeI	GGGCCATATGAACAAAACGCTAATC
agp-R-BamHI	CAGAGGATCCTTATTTCACCGCTTC
yqaB-F-NdeI	GGGCCATATGTACGAGCGTTATG
yqaB-R-BamHI	CAGAGGATCCTCACAGCAAGCGAAC
aphAU-F	TCGCTCATTTGCCGAGGATT
aphA-R403	GGGCTACGACCAGTCACAAA
agpU-F	CAGGTGCAATTATCAGCGGC
agp-R521	GCTGTCGGTAAGCTGGAGTT
yqaBU-F	ACGCAATGGAAAGAAACGCC
yqaB-R243	TATGCTGCTGGATAGCGTCG
PMD-F-NdeI	TATACATATGACCGTTTACACAGCATC
PMD-R-BamHI	CTAGAGGATCCTTATTCCTTTGGTAGAC
PMDse-F-NdeI	TATACATATGGTGAAAAGTGGCAAAGCACG
PMDse-R-BamHI	CTAGAGGATCCTTACTTAATAATTTCAACACCAGAGC
PMDhv-F-NdeI	GATATACATATGAAAGCCACCGCC
PMDhv-R-BamHI	CTAGAGGATCCTTAGAACAGGGCTT
PMDsc-F-K22M	AAGTATTGGGGGATGAGGGACACGAAG
PMDsc-F-S155E	AAGGGGTCTGGTGAAGCTTGTAGATCG
PMDsc-F-S208E	AAGGATGTGAGTGAAACTCAGGGTATG
PMDsc-R-K22M	CTTCGTGTCCCTCATCCCCCAATACTT
PMDsc-R-S155E	CGATCTACAAGCTTCACCAGACCCCTT
PMDsc-R-S208E	CATACCCTGAGTTTCACTCACATCCTT
PMDsc-F-T209D	GATGTGAGTTCCGATCAGGGTATGCAA
PMDsc-R-T209D	TTGCATACCCTGATCGGAACTCACATC
PMDsc-F-I145F	CAGTCAACTTCAGAATTTTCTAGAATAGCAAG
PMDsc-F-R74H	GCATCGACAATGAACATACTCAAAATTGTCTG
PMDsc-R-I145F	CTTGCTATTCTAGAAAATTCTGAAGTTGACTG
PMDsc-R-R74H	CAGACAATTTTGAGTATGTTCATTGTCGATGC